The Astrophysical Journal Supplement Series, 219:27 (19pp), 2015 August doi:10.1088/0067-0049/219/2/27

ASTEROID SPIN-RATE STUDY USING THE INTERMEDIATE PALOMAR TRANSIENT FACTORY

Chan-Kao Chang[1], Wing-Huen Ip[1,2], Hsing-Wen Lin[1], Yu-Chi Cheng[1], Chow-Choong Ngeow[1], Ting-Chang Yang[1], Adam Waszczak[3], Shrinivas R. Kulkarni[4], David Levitan[4], Branimir Sesar[4], Russ Laher[5], Jason Surace[5], and Thomas. A. Prince[4]
[1] Institute of Astronomy, National Central University, Jhongli, Taiwan; rex@astro.ncu.edu.tw
[2] Space Science Institute, Macau University of Science and Technology, Macau, China
[3] Division of Geological and Planetary Sciences, California Institute of Technology, Pasadena, CA 91125, USA
[4] Division of Physics, Mathematics and Astronomy, California Institute of Technology, Pasadena, CA 91125, USA
[5] Spitzer Science Center, California Institute of Technology, M/S 314-6, Pasadena, CA 91125, USA
Received 2015 February 3; accepted 2015 June 27; published 2015 August 11

ABSTRACT

Two dedicated asteroid rotation-period surveys have been carried out in the R band with ∼20 minute cadence using the intermediate Palomar Transient Factory (iPTF) during 2014 January 6–9 and February 20–23. The total survey area covered 174 deg^2 in the ecliptic plane. Reliable rotation periods for 1438 asteroids are obtained from a larger data set of 6551 mostly main-belt asteroids, each with ⩾10 detections. Analysis of 1751, PTF-based, reliable rotation periods clearly shows the spin barrier at ∼2 hr for rubble-pile asteroids. We found a new large super-fast rotator, 2005 UW163, and another five candidates as well. For asteroids of $3 < D < 15$ km, our spin-rate distribution shows a number decrease along with frequency after 5 rev day^{-1}, which is consistent with the results of the Asteroid Light Curve Database. The discrepancy between our work and that of Pravec et al. (update 2014 April 20) comes mainly from asteroids with $\Delta m < 0.2$ mag, which could be the result of different survey strategies. For asteroids with $D < 3$ km, we see a significant number drop at $f = 6$ rev day^{-1}. The relatively short YORP effect timescale for small asteroids could have spun up those elongated objects to reach their spin-rate limit resulting in breakup to create such a number deficiency. We also see that the C-type asteroids show a smaller spin-rate limit than the S-type, which agrees with the general impression that C-type asteroids have a lower bulk density than S-type asteroids.

Key words: minor planets, asteroids: general – surveys

Supporting material: extended figure, machine-readable table

1. INTRODUCTION

Thanks to modern technology—wide-field detectors, high computing power, massive data storage, and robotic observation—it is possible to obtain many asteroid light curves within a short period of time. Therefore, several important physical properties derived from asteroid light curves can be investigated in a more comprehensive way. For instance, the asteroid rotation period (P) is the most direct and essential property for understanding asteroids and the system they populate.

One of the key discoveries from asteroid rotation-period studies is the "spin barrier" at 2.2 hr for asteroids with diameters of (D) > 1 km (Harris 1996), which is crucial evidence supporting the "rubble-pile" model in which it is believed that asteroids are created by gravitationally bounded aggregations and would break up under such super-fast rotation with $P < 2.2$ hr. Pravec & Harris (2000) go a step further to show that the spin barrier can hold for large asteroids (i.e., $D > 150$ m), and other small asteroids, such as coherent monoliths, are able to rotate faster than that limit (i.e., super-fast-rotators, hereafter, SFRs; see the examples in Hergenrother & Whiteley 2011).

In fact, two large SFRs have been discovered: 2001 OE84 ($D \sim 0.65$ km, $P = 29.19$ minutes; Pravec et al. 2002) and 2005 UW163 ($D \sim 0.6$ km, $P = 1.29$ hr; Chang et al. 2014b). One possible explanation for these large SFRs is a size-dependent strength model for asteroids, in which the cohesiveness and tensile strength of an asteroid decrease as its size increases. Therefore, a smooth transition can occur between small monolithic asteroids and large rubble-pile asteroids (Holsapple 2007). In this way, a certain fraction of large SFRs should be found in asteroid populations. Identification of these large SFRs, along with their physical properties, will provide definite answers about this special asteroid group.

Another notable discovery from analyzing asteroid rotation periods is that the spin-rate distribution of smaller asteroids (i.e., $3 < D < 15$ km) have excesses in both the slow and fast ends. When an asteroid system reaches collisional equilibrium, it exhibits a Maxwellian spin-rate distribution (Salo 1987), which has been observed for asteroids of $D > 40$ km (Pravec et al. 2002). Therefore, the excesses of slow- and fast-rotating small asteroids become clear evidence of the Yarkovsky–O'Keefe–Radzievskii–Paddack (YORP) effect altering the spin rate of small asteroids on million-year timescales (Rubincam 2000). However, the spin-rate distribution of small asteroids is still under debate. Instead of the flat distribution reported by Pravec et al. (2008), a non-flat distribution (i.e., more closely resembling a Maxwellian distribution) was found by Masiero et al. (2009), Polishook & Brosch (2009), and Chang et al. (2014a). Although the YORP effect can account for both cases, a detailed investigation is still needed to understand the spin-rate evolution of small asteroids.

Moreover, rubble-pile asteroids with a lower bulk density (ρ) should have a smaller spin-rate limit ($P \sim 3.3\sqrt{(1+\Delta m)/\rho}$; Pravec & Harris 2000). Consequently, the overall spin rate of C-type asteroids (i.e., $\rho \sim 1.33 \pm 0.58$ g cm^{-3}) should be lower than for S-types (i.e., $\rho \sim 2.72 \pm 0.54$ g cm^{-3}; DeMeo & Carry 2013). Although Chang et al. (2014a) attempted to investigated whether or not this trend exists between various

spectral-type asteroids, the conclusion was still preliminary due to the availability of only a few tens of objects in their samples.

To gain a more comprehensive understanding with respect to the aforementioned questions, we continued our previous study and conducted two more asteroid rotation-period surveys of data taken on 2014 January 6–9 and February 20–23 by the intermediate Palomar Transient Factory (iPTF).[6] These surveys included more samples and a higher level of completeness. The total survey area was $\sim$174 deg^2 over the ecliptic plane and 6551 asteroids of $\geqslant$10 detections were obtained. From these light curves, 1438 reliable rotation periods were derived, among which we found 6 large SFR candidates, 1 of which ((335,433) 2005 UW163) was confirmed via follow-up observation (Chang et al. 2014b).

We describe our observation information and light-curve extraction in Section 2. Our periodicity analysis is provided in Section 3. The results and discussion are presented in Section 4. A summary and conclusion can be found in Section 5.

2. OBSERVATIONS AND DATA REDUCTION

The PTF project, and its successor the iPTF project, employs the Palomar 48 inch Oschin Schmidt Telescope equipped with an 11-chip mosaic CCD camera to explore synoptically the transient and variable sky. This configuration creates a field of view of $\sim$7.26 deg^2 and a pixel scale of 1.″01 (Law et al. 2009; Rau et al. 2009). Most PTF exposures are taken in the Mould-R band, and the other available filters are the Gunn-g' and two different H_α bands. A 60 s R-band exposure can reach a median limiting magnitude of $\sim$21 mag at the 5σ level (Law et al. 2010).

Each PTF exposure is processed by the IPAC-PTF photometric pipeline, which includes image splitting, debiasing, flat-fielding, source extraction, astrometric calibration, and photometric calibration to generate reduced images and source catalogs (Grillmair et al. 2010; Laher et al. 2014). The absolute magnitude calibration is done against Sloan Digital Sky Survey fields (hereafter, SDSS; York et al. 2000) on a per-night, per-filter, per-chip basis, and routinely reaches a precision of $\sim$0.02 mag on photometric nights (Ofek et al. 2012a, 2012b). Small photometric zero-point variations are possible between catalogs of different nights, fields, filters, and chips. Its accuracy depends on what degree it is affected by weather and transient variations in atmospheric conditions in a night.

To collect a large sample of asteroid light curves to further our previous asteroid spin-rate studies (Polishook et al. 2012; Chang et al. 2014a), we conducted two asteroid rotation-period surveys during 2014 January 6–9 and February 20–23. Each survey continuously scanned 12 consecutively numbered PTF fields in the ecliptic plane in the R band with a cadence of $\sim$20 minutes. The exposure time of each frame was 60 s, and the scanned sky coverage was $\sim$174 deg^2 in total. The observational metadata are given in Table 1 and the field configurations are shown Figure 1. After purging all stationary sources, the source catalogs were matched against the ephemerides obtained from the *JPL/HORIZONS* system with a radius of 2″ to extract the light curves of known asteroids. We also excluded any detection flagged as a defect by the IPAC-PTF photometric pipeline from the light curves. In the end, we were left with 6551 asteroid light curves, each with $\geqslant$10 data points (hereafter, PTF-detected asteroids), for the following rotation-period analysis.

Table 1
Survey Observations in 2014 January

Field ID	R.A. (°)	decl. (°)	Jan 6 Δt, $N_{\rm exp}$	Jan 7 Δt, $N_{\rm exp}$	Jan 8 Δt, $N_{\rm exp}$	Jan 9 Δt, $N_{\rm exp}$
3559	117.00	19.12	9.6, 28	9.8, 30	5.1, 16	9.7, 12
3560	120.60	19.12	9.7, 29	9.8, 30	5.1, 16	9.7, 12
3561	124.20	19.12	9.3, 28	9.4, 29	5.5, 17	9.6, 11
3562	127.80	19.12	9.3, 28	9.1, 28	5.5, 17	8.2, 11
3563	131.40	19.12	9.2, 28	8.8, 27	5.1, 16	8.2, 9
3564	135.00	19.12	8.9, 27	8.7, 27	5.1, 16	8.2, 9
3565	138.60	19.12	8.5, 26	8.4, 26	5.1, 16	7.8, 8
3658	115.71	21.38	9.7, 29	9.8, 30	5.1, 16	9.7, 10
3659	119.39	21.38	9.7, 28	9.8, 30	5.1, 16	9.8, 10
3660	123.06	21.38	9.6, 29	9.4, 29	5.1, 16	10.0, 11
3661	126.73	21.38	9.3, 28	9.5, 29	5.1, 16	9.8, 10
3662	130.41	21.38	9.3, 28	9.1, 28	5.1, 16	7.8, 9
Field ID	**R.A. (°)**	**decl. (°)**	**Feb 20 Δt, $N_{\rm exp}$**	**Feb 21 Δt, $N_{\rm exp}$**	**Feb 22 Δt, $N_{\rm exp}$**	**Feb 23 Δt, $N_{\rm exp}$**
3158	143.65	10.12	7.9, 19	7.6, 22	7.9, 22	7.2, 20
3159	147.12	10.12	8.0, 17	7.3, 20	7.9, 21	7.7, 22
3160	150.58	10.12	7.6, 18	7.7, 21	7.7, 22	7.7, 22
3161	154.04	10.12	8.0, 20	8.0, 22	7.9, 23	7.9, 23
3162	157.50	10.12	8.3, 20	7.9, 22	8.0, 24	7.9, 23
3163	160.96	10.12	8.0, 19	7.8, 22	8.0, 24	8.0, 24
3261	141.55	12.38	7.7, 20	7.6, 21	8.2, 23	7.1, 20
3262	145.05	12.38	8.1, 20	7.9, 23	8.2, 23	7.5, 20
3263	148.54	12.38	8.2, 20	7.6, 22	8.1, 23	7.7, 21
3264	152.04	12.38	7.9, 20	8.0, 23	8.2, 24	8.2, 24
3265	155.53	12.38	8.7, 19	8.0, 22	8.1, 24	8.2, 23
3266	159.03	12.38	8.0, 21	8.2, 23	8.1, 25	8.2, 24

Note. Δt is the duration of time spanned by each observing set in hours and $N_{\rm exp}$ is the total number of exposures for each night and field.

3. ROTATION-PERIOD ANALYSIS

Before measuring rotation periods, the orbital elements obtained from the Minor Planet Center[7] were used to correct for light-travel time and to reduce the magnitudes to both heliocentric, r, and geocentric, Δ, distances at 1 AU for all PTF-detected asteroids. Moreover, the absolute magnitudes, H_R, were simply estimated by applying a fixed G_R slope of 0.15 in the H–G system (Bowell et al. 1989, p. 524) due to the small change in phase angles within our four-night observations.

We followed the traditional second-order Fourier series method to fit our light curves (Harris et al. 1989):

$$M_{i,j} = \sum_{k=1,2}^{N_k} B_k \sin\left[\frac{2\pi k}{P}(t_j - t_0)\right] + C_k \cos\left[\frac{2\pi k}{P}(t_j - t_0)\right] + Z_i, \quad (1)$$

where $M_{i,j}$ is the R-band reduced magnitude measured at the light-travel time corrected epoch t_j, B_k and C_k are the Fourier coefficients, P is the rotation period, and t_0 is an arbitrary epoch. Here, we also introduced a constant value Z_i to correct the small photometric zero-point variations between data

[6] Intermediate Palomar Transient Factory: http://ptf.caltech.edu/iptf.

[7] http://minorplanetcenter.net

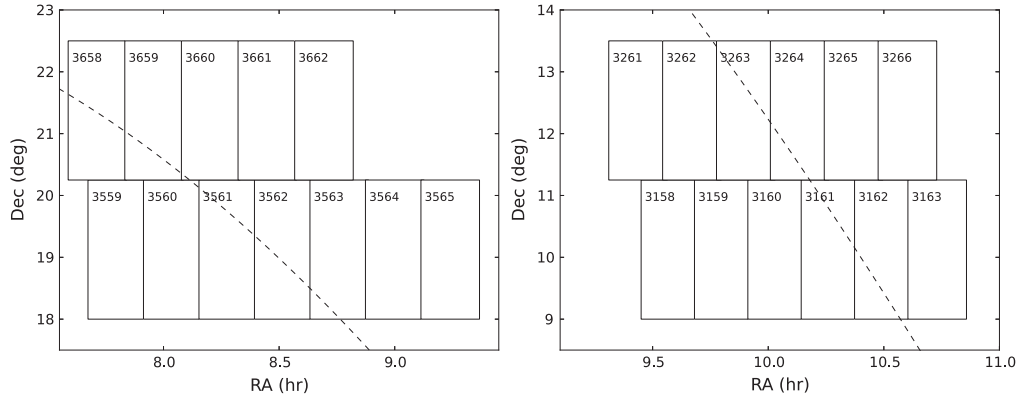

Figure 1. Field configurations for survey data taken in January (left) and February (right) of 2014. The rectangles show PTF fields with corresponding field IDs. The dashed line shows the position of the ecliptic plane. Note that the scales of R.A. and decl. are different.

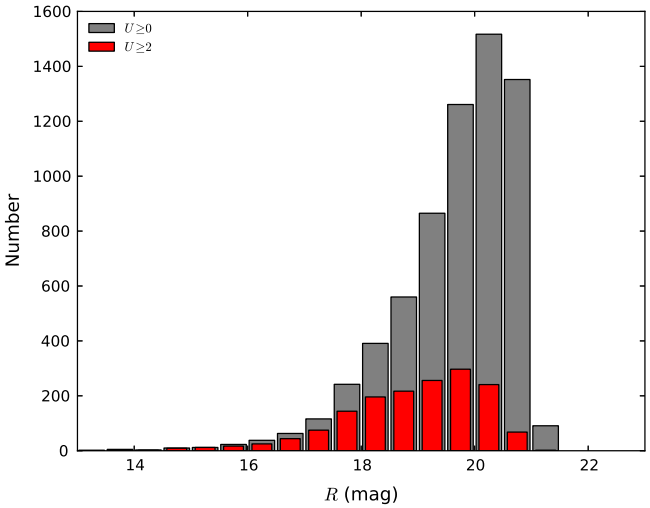

Figure 2. Magnitude distributions of PTF-detected asteroids (gray, $U > 0$) vs. PTF-U2s (red, $U \geqslant 2$). Values of quality code U are defined in Section 3.

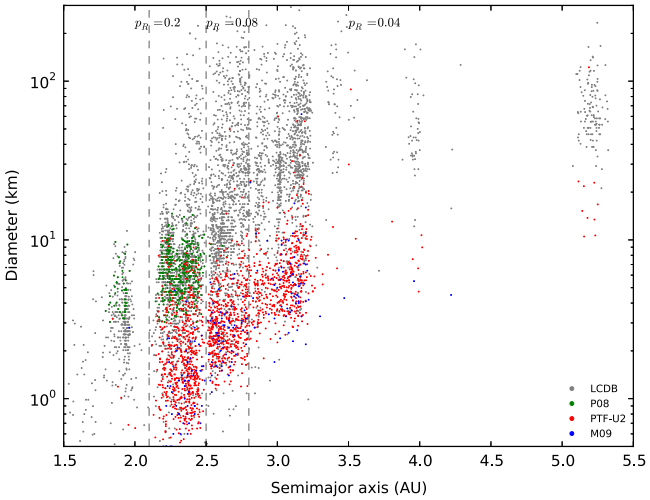

Figure 3. Diameter vs. semimajor axes for PTF-U2s (red), P08 (update 2014 April 20, green), M09 (blue), and LCDB (gray). The dashed lines show the divisions of empirical geometric albedo (p_R) for asteroids located at different regions of the semimajor axis.

acquired from different nights, fields, filters, and chips. Then, Equation (1) was solved by using least-squares minimization for each given P to obtain other free parameters. The spin-rate (f) range was stepped through from 0.25 to 25 rev day^{-1} (e.g., about 1–96 hr) with increments of 0.025 rev day^{-1}.

The results were reviewed and a quality code (U) was manually assigned to each folded light curve, where "3" means highly reliable, "2" means some ambiguity; and "1" means possible but may be wrong (Warner et al. 2009). Moreover, when the light curve was unable to find any acceptable solution, it was assigned $U = 0$. The uncertainty of the derived rotation period was estimated from periods having χ^2 smaller than $\chi^2_{\rm best} + \Delta\chi^2$, where $\chi^2_{\rm best}$ is the χ^2 of the derived period and $\Delta\chi^2$ is calculated from the inverse χ^2 distribution, assuming $1 + 2N_k + N_i$ degrees of freedom. The amplitude was calculated from the peak-to-peak variations after rejecting the upper and lower 5% of data points to avoid outliers, which are probably contaminated by nearby bright stars or unfiltered artifacts from the light-curve extraction.

4. RESULTS AND DISCUSSION

Most PTF-detected asteroids are main-belt asteroids, and the others include Hilda, Jovian Trojan, and near-Earth objects. If the object is available in the *WISE*/*NEOWISE* data set (Grav et al. 2011; Mainzer et al. 2011; Masiero et al. 2011), then we adopted its diameter estimation. Otherwise, the diameter was estimated using

$$D = \frac{1130}{\sqrt{p_R}} 10^{-H_R/5}, \quad (2)$$

where D is the diameter in kilometers, p_R is the R-band geometric albedo, and 1130 is the conversion constant adopted from Jewitt et al. (2013). We assumed three empirical albedo values, $p_R = 0.20$, 0.08, and 0.04, for objects in inner- ($2.1 < a < 2.5$ AU), mid- ($2.5 < a < 2.8$ AU) and outer- ($a > 2.8$ AU) main belts, respectively (Tedesco et al. 2005).

4.1. Derived Rotation Periods

From PTF-detected asteroids, we obtained 1438 reliable (i.e., $U \geqslant 2$) rotation periods (hereafter, PTF-U2s). The magnitude distributions of the PTF-detected asteroids versus PTF-U2s are shown in Figure 2, which peak at ~20.5 and ~19.5 mag, respectively. Figure 3 shows the plot of the semimajor axis versus diameter for PTF-U2s, where we see the low-limit diameters increasing as a function of semimajor axis. The derived rotation periods and light-curve amplitudes, along with

Table 2
Synodic Rotation Periods of PTF-U2s

Obj ID	Designation	a	e	i	Ω	ω	D	$\triangle$	r	α	H_R	n	m	PTF_R	Period (hr)	$\triangle m$	U
00414[a]	(414) Liriope	3.52	0.07	9.56	110.6	322.7	88.8[c]	3.32	2.35	3.38	9.22 ± 0.12	4	81	13.99 ± 0.00	7.38 ± 0.11	0.14	2
00659[a]	(659) Nestor	5.19	0.11	4.52	350.9	342.0	122.3[c]	5.78	4.79	0.70	8.47 ± 0.13	4	89	15.78 ± 0.00	16.00 ± 0.26	0.22	3
01098[a]	(1098) Hakone	2.69	0.12	13.38	329.0	81.4	29.6[c]	2.70	1.72	2.89	10.35 ± 0.12	2	43	13.94 ± 0.00	7.16 ± 0.05	0.35	3
01117[a]	(1117) Reginita	2.25	0.20	4.34	147.1	151.1	10.2[c]	2.58	1.60	1.03	11.47 ± 0.07	2	48	14.70 ± 0.00	2.94 ± 0.01	0.11	3
01153[a]	(1153) Wallenbergia	2.20	0.16	3.34	280.6	28.9	9.9	2.52	1.54	3.64	12.04 ± 0.10	1	22	15.22 ± 0.00	4.12 ± 0.07	0.23	2
01254[a]	(1254) Erfordia	3.14	0.03	7.07	288.0	239.4	56.1[c]	3.08	2.10	1.88	10.23 ± 0.12	3	68	14.58 ± 0.00	12.31 ± 0.16	0.33	3
01443[a]	(1443) Ruppina	2.94	0.06	1.93	174.9	163.7	17.2[c]	3.12	2.14	2.33	10.97 ± 0.12	4	85	15.21 ± 0.00	5.89 ± 0.04	0.27	3
01470[a]	(1470) Carla	3.16	0.07	3.21	358.5	342.5	34.1[c]	3.37	2.38	0.89	10.80 ± 0.12	4	107	15.49 ± 0.00	6.15 ± 0.04	0.24	3
01476	(1476) Cox	2.28	0.19	6.33	330.6	350.1	7.4[c]	2.71	1.73	2.69	12.87 ± 0.10	4	85	16.47 ± 0.01	3.86 ± 0.02	0.13	3
01497	(1497) Tampere	2.90	0.08	1.06	300.3	29.6	16.3[c]	3.07	2.09	2.04	11.30 ± 0.12	4	76	15.57 ± 0.00	3.30 ± 0.01	0.20	3

Notes. Columns: asteroid's designations, semimajor axis (a, AU), eccentricity (e, degree), inclination (i, degree), longitude of ascending node (Ω, degree), argument of periapsis (ω, degree), diameter (D, kilometers), heliocentric distance ($\triangle$, AU), geodesic distance (r, AU), phase angle (α, degree), absolute magnitude (H, mag), number of nights (n), number of images (m), PTF_R magnitude, derived rotation period (hours), light-curve amplitude (mag), and rotation-period quality code (U).

[a] Asteroid available in the LCDB.

[b] Light curves with large amplitudes and deep V-shape minima.

[c] *WISE*/*NEOWISE* diameter.

(This table is available in its entirety in machine-readable form.)

Table 3
Asteroids with Partial Phase Coverage

Obj ID	Designation	a	e	i	Ω	ω	D	$\triangle$	r	α	H_R	n	m	PTF$_R$	Period (hr)	$\triangle m$	U
00850[a]	(850) Altona	3.01	0.12	15.53	121.2	133.5	59.9[c]	3.24	2.30	6.02	9.37 ± 0.13	4	86	14.11 ± 0.00	11.16 ± 0.38	0.10	2
01100[a]	(1100) Arnica	2.90	0.07	1.03	304.2	23.8	17.2[c]	3.06	2.08	3.05	10.39 ± 0.11	4	79	14.77 ± 0.00	14.55 ± 0.22	0.09	2
01135[a]	(1135) Colchis	2.67	0.12	4.54	350.8	4.1	49.8[c]	2.95	1.96	1.28	10.26 ± 0.18	4	77	14.21 ± 0.00	23.41 ± 1.09	0.33	2
01449[a]	(1449) Virtanen	2.22	0.14	6.64	110.8	131.9	9.9[c]	2.36	1.42	9.32	11.69 ± 0.15	4	64	14.92 ± 0.00	14.77 ± 0.44	0.27	2
02009[a]	(2009) Voloshina	3.12	0.14	2.86	107.6	6.3	26.6[c]	2.75	1.76	1.27	10.87 ± 0.12	4	88	14.59 ± 0.00	2.94 ± 0.01	0.32	2
03014[a]	(3014) Huangsushu	2.36	0.23	0.99	140.8	180.6	6.9[c]	2.89	1.90	0.78	13.15 ± 0.15	3	68	16.96 ± 0.01	24.00 ± 0.62	0.35	2
03031[a]	(3031) Houston	2.24	0.10	4.34	317.8	249.1	6.8[c]	2.11	1.12	4.17	12.81 ± 0.08	4	62	15.06 ± 0.00	5.61 ± 0.06	0.17	2
03033[a]	(3033) Holbaek	2.24	0.09	4.74	166.9	67.3	9.1[c]	2.19	1.20	1.81	12.68 ± 0.09	4	82	14.97 ± 0.00	20.00 ± 0.87	0.15	2
03484	(3484) Neugebauer	2.59	0.18	15.37	116.1	176.1	6.9[c]	3.07	2.11	5.47	12.75 ± 0.11	4	97	17.20 ± 0.01	12.63 ± 0.32	0.10	2
04471	(4471) Graculus	2.86	0.16	13.87	345.5	43.3	11.7[c]	3.10	2.12	1.99	11.90 ± 0.19	1	17	16.34 ± 0.01	11.85 ± 75.42	0.49	2
04746	(4746) Doi	3.22	0.17	0.88	185.4	212.1	20.3[c]	3.01	2.04	3.73	12.03 ± 0.08	2	58	16.26 ± 0.01	20.43 ± 0.43	0.24	2
05008	(5008) Miyazawakenji	2.22	0.06	5.27	142.4	41.8	7.8[c]	2.10	1.11	1.72	12.79 ± 0.10	4	97	14.72 ± 0.00	13.52 ± 0.19	0.18	2
05450	(5450) Sokrates	2.81	0.12	5.23	145.2	318.9	23.6[c]	2.55	1.56	1.76	12.22 ± 0.06	1	19	15.40 ± 0.00	2.98 ± 0.06	0.21	2
05535[a]	(5535) Annefrank	2.21	0.06	4.25	120.7	9.0	4.7	2.08	1.10	3.55	13.65 ± 0.12	3	71	15.74 ± 0.00	21.33 ± 0.99	0.20	2
05833	(5833) Peterson	3.50	0.03	19.36	306.7	120.1	29.9[c]	3.43	2.49	5.18	10.82 ± 0.14	4	72	15.98 ± 0.00	27.43 ± 0.81	0.24	2
06902	(6902) Hideoasada	2.75	0.10	2.09	214.2	129.2	9.5	3.02	2.04	1.98	13.12 ± 0.14	4	92	17.32 ± 0.01	15.00 ± 0.24	0.36	2
08568	(8568) Larrywilson	2.16	0.10	0.87	44.7	242.4	3.1[c]	2.30	1.31	0.92	15.08 ± 0.16	4	87	17.61 ± 0.02	11.29 ± 0.13	0.39	2
09369	(9369) 1993 DB1	2.33	0.15	0.22	97.3	107.2	4.6[c]	2.26	1.31	7.76	13.62 ± 0.13	4	78	16.51 ± 0.01	14.12 ± 0.21	0.17	2
09457	(9457) 1998 FB75	3.17	0.18	0.47	32.1	51.8	11.7[c]	2.68	1.72	5.26	13.07 ± 0.19	4	84	16.80 ± 0.01	22.86 ± 0.56	0.36	2
09655	(9655) 1996 CH1	2.37	0.07	4.97	120.6	327.8	3.4[c]	2.22	1.26	7.35	13.78 ± 0.11	4	82	16.53 ± 0.01	6.67 ± 0.05	0.14	2
10792	(10792) Ecuador	3.07	0.09	10.27	157.2	177.7	10.1[c]	3.35	2.36	0.52	12.79 ± 0.27	4	85	17.41 ± 0.02	18.82 ± 0.36	0.90	2
10816	(10816) 1993 FZ35	3.15	0.14	2.65	116.4	217.7	10.2[c]	3.49	2.53	4.53	13.58 ± 0.16	4	72	18.68 ± 0.04	14.12 ± 0.40	0.47	2
11187	(11187) Richoliver	2.59	0.13	3.86	131.0	151.6	3.9[c]	2.76	1.78	1.86	14.07 ± 0.14	4	85	17.71 ± 0.02	14.55 ± 0.45	0.45	2
11286	(11286) 1990 RO8	2.38	0.14	3.20	159.3	324.4	3.8[c]	2.08	1.09	2.45	14.61 ± 0.17	3	57	16.64 ± 0.01	10.67 ± 0.23	0.44	2
11775	(11775) Kohler	2.17	0.03	3.37	164.9	245.0	2.4	2.18	1.20	2.47	15.08 ± 0.11	2	43	17.40 ± 0.01	8.21 ± 0.14	0.37	2
12117	(12117) Meagmessina	2.47	0.18	3.07	158.3	19.0	3.1[c]	2.07	1.08	3.04	14.53 ± 0.19	4	85	16.58 ± 0.01	14.33 ± 0.21	0.66	2
12793	(12793) 1995 UP8	2.26	0.14	3.37	355.0	291.5	3.4[c]	2.44	1.45	1.69	14.37 ± 0.21	4	88	17.29 ± 0.01	12.63 ± 0.17	0.54	2
13187	(13187) 1997 AN4	2.27	0.14	0.97	286.0	311.3	3.7[c]	2.39	1.43	7.49	15.24 ± 0.14	4	78	18.44 ± 0.03	12.97 ± 0.55	0.20	2
13323	(13323) 1998 SQ	5.11	0.09	0.92	182.5	256.0	23.4[c]	4.97	3.98	0.49	11.01 ± 0.13	4	79	17.57 ± 0.02	14.77 ± 0.44	0.27	2
13580	(13580) de Saussure	2.82	0.23	5.82	294.0	79.5	6.4[c]	2.75	1.77	2.27	13.91 ± 0.10	4	80	17.56 ± 0.02	12.31 ± 0.32	0.17	2
13717	(13717) Vencill	2.28	0.05	2.23	212.1	30.1	2.5[c]	2.28	1.30	3.64	15.40 ± 0.13	4	77	18.13 ± 0.02	24.00 ± 2.18	0.33	2
14779	(14779) 3072 T-2	2.84	0.07	3.20	83.6	243.4	6.8[c]	3.03	2.05	1.90	13.23 ± 0.18	3	63	17.36 ± 0.01	17.78 ± 0.32	0.50	2
15075	(15075) 1999 BF15	2.40	0.20	1.87	206.9	182.9	4.1[c]	2.56	1.58	1.92	14.03 ± 0.11	4	79	17.29 ± 0.01	16.00 ± 0.55	0.14	2
15352	(15352) 1994 VB7	2.39	0.16	2.81	223.2	197.3	2.9[c]	2.32	1.34	4.65	15.03 ± 0.13	4	76	17.86 ± 0.02	12.63 ± 0.17	0.30	2
15670	(15670) 1975 SO1	3.01	0.04	2.38	145.1	334.6	10.2	2.90	1.91	1.40	13.72 ± 0.10	4	104	17.55 ± 0.02	21.33 ± 0.46	0.23	2
18188	(18188) 2000 QD55	3.10	0.23	3.37	51.9	301.3	7.7[c]	3.77	2.79	1.56	14.30 ± 0.20	4	70	19.62 ± 0.08	11.85 ± 0.29	0.58	2
18647	(18647) Vaclavhubner	2.54	0.04	3.72	141.2	39.1	2.7[c]	2.44	1.45	0.91	15.29 ± 0.17	4	83	18.16 ± 0.03	33.10 ± 2.14	0.56	2
19210	(19210) 1992 YE4	2.58	0.23	4.09	150.4	240.8	4.7	2.73	1.74	2.82	14.62 ± 0.09	4	73	18.20 ± 0.03	6.23 ± 0.08	0.17	2
20106	(20106) Morton	2.65	0.16	13.35	323.1	104.3	3.2[c]	2.52	1.53	2.61	14.94 ± 0.14	4	70	18.20 ± 0.03	8.97 ± 0.08	0.20	2
20116	(20116) 1995 VE1	2.68	0.10	3.02	104.6	271.1	3.9	2.69	1.71	3.52	15.06 ± 0.28	4	74	18.56 ± 0.04	14.77 ± 0.47	0.84	2
21119	(21119) 1992 UJ	2.54	0.19	2.37	307.7	96.0	5.7[c]	2.57	1.58	3.08	14.96 ± 0.22	2	41	18.41 ± 0.04	12.97 ± 0.18	0.70	2
23184	(23184) 2000 OD36	2.41	0.21	21.82	152.8	121.9	9.0[c]	2.56	1.58	1.89	14.01 ± 0.32	4	80	17.27 ± 0.02	29.09 ± 0.91	1.20	2
24615	(24615) 1978 VO5	2.29	0.11	2.58	271.9	120.1	2.2[c]	2.23	1.25	4.77	15.09 ± 0.12	4	70	17.67 ± 0.02	11.03 ± 0.25	0.21	2
24856	(24856) Messidoro	2.72	0.25	8.80	159.7	304.1	4.5[c]	2.16	1.19	6.61	15.07 ± 0.09	2	40	17.63 ± 0.02	2.39 ± 0.02	0.20	2
25014	(25014) Christinepalau	2.24	0.18	4.63	326.8	293.5	4.0[c]	2.31	1.32	1.61	14.55 ± 0.12	4	82	17.09 ± 0.01	12.00 ± 0.43	0.15	2
25469	(25469) Ransohoff	2.32	0.14	7.56	108.4	263.6	3.7[c]	2.36	1.39	6.11	14.19 ± 0.13	4	70	17.21 ± 0.01	8.57 ± 0.15	0.11	2
26138	(26138) 1993 TK25	2.79	0.10	3.30	179.1	141.7	3.7[c]	3.05	2.06	2.20	15.36 ± 0.36	4	71	19.60 ± 0.07	32.00 ± 3.56	1.26	2
29146	(29146) McHone	2.40	0.24	23.63	333.9	203.7	3.8[c]	1.85	0.86	0.85	14.13 ± 0.10	3	63	15.22 ± 0.00	14.12 ± 0.40	0.18	2

Table 3
(Continued)

Obj ID	Designation	a	e	i	Ω	ω	D	$\triangle$	r	α	H_R	n	m	PTF_R	Period (hr)	$\triangle m$	U
29219	(29219) 1992 BJ	2.36	0.13	2.92	124.6	334.0	6.3[c]	2.16	1.17	1.32	14.77 ± 0.09	3	60	16.91 ± 0.01	12.00 ± 0.71	0.09	2
29536	(29536) 1998 BC12	3.04	0.03	11.62	110.7	344.9	9.6[c]	2.94	1.98	4.88	12.74 ± 0.17	4	51	16.98 ± 0.01	7.22 ± 0.11	0.16	2
30111	(30111) 2000 FJ20	2.36	0.09	7.08	109.2	155.0	2.2	2.52	1.58	8.83	15.29 ± 0.20	3	65	18.89 ± 0.04	8.65 ± 0.16	0.63	2
30343	(30343) 2000 JB36	2.37	0.16	2.29	359.3	202.6	2.7[c]	2.24	1.32	11.44	14.68 ± 0.15	4	65	17.72 ± 0.02	7.56 ± 0.25	0.16	2
30455	(30455) 2000 NB27	3.09	0.01	10.37	311.4	105.0	7.2[c]	3.08	2.18	8.58	13.19 ± 0.09	2	52	17.91 ± 0.02	7.87 ± 0.13	0.32	2
30971	(30971) 1995 DJ	2.44	0.28	7.80	337.5	56.4	4.3	2.64	1.65	1.44	13.83 ± 0.27	4	86	17.48 ± 0.02	32.00 ± 1.10	0.68	2
31021	(31021) 1996 FW1	2.36	0.17	1.49	133.2	95.2	2.9[c]	2.18	1.19	2.66	15.30 ± 0.34	3	62	17.48 ± 0.01	19.20 ± 0.80	0.68	2
31987	(31987) 2000 HN28	2.42	0.21	1.46	307.1	38.6	1.9	2.73	1.79	7.88	15.62 ± 0.26	4	62	19.60 ± 0.08	9.70 ± 0.10	0.97	2
32281	(32281) 2000 PP21	3.03	0.08	1.45	349.2	291.3	5.7	3.16	2.17	0.43	14.99 ± 0.13	4	76	19.17 ± 0.05	13.15 ± 0.37	0.37	2
32358	(32358) 2000 QS124	3.12	0.07	18.05	150.7	341.0	6.9[c]	2.91	1.94	4.37	13.37 ± 0.11	4	81	17.49 ± 0.01	21.82 ± 0.51	0.28	2
39297	(39297) 2001 FE53	2.73	0.07	2.25	30.6	284.0	4.5	2.90	1.92	1.42	14.76 ± 0.14	4	85	18.60 ± 0.04	6.91 ± 0.05	0.33	2
45837	(45837) 2000 RD27	2.46	0.14	14.21	325.9	324.1	3.6[c]	2.69	1.71	2.03	14.91 ± 0.26	4	79	18.40 ± 0.03	32.00 ± 2.29	0.79	2
46165[b]	(46165) 2001 FF80	2.72	0.22	7.66	291.0	217.7	5.4[c]	2.19	1.23	7.38	14.58 ± 0.12	4	80	17.22 ± 0.01	11.03 ± 0.13	0.20	3
46769	(46769) 1998 HJ2	2.21	0.15	3.53	122.7	185.9	1.5	2.51	1.52	1.33	16.11 ± 0.19	4	80	18.92 ± 0.05	32.00 ± 5.33	0.62	2
47340	(47340) 1999 XK39	2.25	0.12	3.37	157.3	222.8	1.8[c]	2.40	1.42	2.11	15.65 ± 0.22	4	82	18.44 ± 0.04	40.00 ± 3.08	0.79	2
48476	(48476) 1991 UP3	2.35	0.20	3.21	87.0	320.9	1.8[c]	2.13	1.21	11.93	15.48 ± 0.11	4	90	18.20 ± 0.02	6.81 ± 0.10	0.18	2
48835	(48835) 1997 YK18	3.00	0.09	10.71	146.4	287.7	10.7	2.92	1.94	0.78	13.61 ± 0.13	4	83	17.49 ± 0.02	32.00 ± 3.56	0.38	2
49889	(49889) 1999 XA158	2.26	0.06	4.27	142.0	46.0	4.9[c]	2.14	1.15	1.17	15.29 ± 0.09	4	85	17.41 ± 0.02	7.06 ± 0.10	0.10	2
51495[b]	(51495) 2001 FO79	2.25	0.15	6.30	293.4	309.0	3.7[c]	2.41	1.45	5.95	15.03 ± 0.20	4	81	18.21 ± 0.03	8.97 ± 0.17	0.71	3
52199	(52199) 2465 T-3	2.33	0.13	2.11	295.4	138.4	1.9[c]	2.10	1.15	8.61	15.63 ± 0.36	3	37	18.24 ± 0.03	6.04 ± 0.04	0.82	2
53186	(53186) 1999 CB45	2.97	0.06	11.51	121.0	9.8	5.6[c]	2.81	1.85	5.29	13.86 ± 0.20	1	28	17.82 ± 0.02	6.67 ± 0.22	0.63	2
54272	(54272) 2000 JT40	2.90	0.04	2.20	163.0	111.9	5.3	2.95	1.97	1.32	15.13 ± 0.19	3	48	19.06 ± 0.06	16.27 ± 0.79	0.61	2
55025	(55025) 2001 QF40	2.90	0.08	1.73	349.6	8.7	3.4[c]	3.12	2.13	0.49	14.84 ± 0.16	4	81	19.10 ± 0.06	15.24 ± 1.03	0.53	2
55860	(55860) 1997 BQ6	3.20	0.12	0.91	57.9	98.1	5.6[c]	2.86	1.92	6.61	15.45 ± 0.24	4	75	19.63 ± 0.08	11.85 ± 0.29	0.72	2
55917	(55917) 1998 FN30	3.08	0.13	10.70	346.1	299.0	5.0[c]	3.30	2.31	1.34	14.01 ± 0.10	4	79	18.58 ± 0.04	9.41 ± 0.18	0.34	2
56005[b]	(56005) 1998 SK169	2.77	0.17	10.02	153.4	201.1	4.2	3.14	2.17	4.59	14.91 ± 0.18	4	70	19.44 ± 0.06	7.33 ± 0.06	0.78	3
59408	(59408) 1999 FL40	2.42	0.20	2.05	295.5	175.6	1.9	2.01	1.03	5.29	15.61 ± 0.09	4	82	17.49 ± 0.02	7.50 ± 0.12	0.20	2
61679	(61679) 2000 QH124	3.18	0.14	6.52	150.7	274.5	6.3	3.07	2.08	1.71	14.77 ± 0.16	3	57	18.98 ± 0.05	13.71 ± 0.91	0.40	2
62606	(62606) 2000 SK325	3.19	0.14	12.72	344.4	96.1	5.6	3.02	2.03	1.60	15.04 ± 0.38	4	81	19.26 ± 0.06	16.27 ± 0.27	1.15	2
63475	(63475) 2001 OB32	3.00	0.11	8.65	303.9	95.4	5.8[c]	2.89	1.94	5.69	13.95 ± 0.13	4	76	18.14 ± 0.02	12.47 ± 0.32	0.22	2
64036	(64036) 2001 SO190	2.38	0.13	1.47	153.5	318.6	1.1	2.11	1.13	3.52	16.83 ± 0.22	3	55	19.00 ± 0.06	11.29 ± 0.26	0.64	2
64372[b]	(64372) 2001 UQ113	2.40	0.17	0.22	146.4	88.4	2.0	2.55	1.58	4.99	15.50 ± 0.10	4	82	18.73 ± 0.04	9.60 ± 0.19	0.26	2
64419	(64419) 2001 UG186	2.42	0.09	5.95	309.9	161.5	1.4	2.20	1.26	10.58	16.35 ± 0.17	4	71	19.24 ± 0.07	14.33 ± 0.67	0.48	2
65821	(65821) 1996 UC3	4.01	0.23	4.31	302.3	103.6	10.7	3.57	2.63	4.91	13.61 ± 0.30	4	66	18.82 ± 0.05	6.44 ± 0.04	0.71	2
66067	(66067) 1998 RM19	2.75	0.15	6.12	351.8	72.0	5.4[c]	2.68	1.70	1.29	14.78 ± 0.18	4	93	18.23 ± 0.03	10.32 ± 0.11	0.49	2
66468	(66468) 1999 RL17	2.67	0.13	2.88	256.0	183.4	4.1	2.37	1.39	4.09	14.92 ± 0.18	4	79	17.87 ± 0.03	30.00 ± 3.33	0.43	2
67357	(67357) 2000 KS15	2.95	0.02	3.23	87.2	163.3	5.3	2.99	2.09	8.70	15.15 ± 0.25	3	61	19.68 ± 0.08	8.35 ± 0.07	0.82	2
69561	(69561) 1997 YD2	2.17	0.06	4.37	286.6	246.1	1.9	2.09	1.12	6.13	15.61 ± 0.32	3	69	17.79 ± 0.02	43.64 ± 4.36	0.97	2
69926	(69926) 1998 TZ31	2.84	0.19	3.81	286.3	113.7	5.3[c]	2.63	1.67	5.88	14.86 ± 0.11	4	74	18.59 ± 0.04	22.86 ± 2.43	0.28	2
70740	(70740) 1999 VG18	2.66	0.15	1.56	288.0	74.9	4.4[c]	2.95	1.97	3.68	15.81 ± 0.24	4	60	19.99 ± 0.11	4.53 ± 0.02	0.76	2
70741	(70741) 1999 VO18	2.69	0.05	1.65	305.2	118.5	3.1[c]	2.61	1.67	7.96	14.81 ± 0.11	4	68	18.56 ± 0.04	13.33 ± 0.38	0.33	2
71441	(71441) 2000 AR226	2.79	0.08	5.27	107.8	278.5	4.6[c]	2.75	1.77	2.36	15.05 ± 0.13	4	67	18.72 ± 0.05	10.43 ± 0.22	0.36	2
74103	(74103) 1998 QP31	2.31	0.08	6.49	107.6	31.4	2.7[c]	2.14	1.16	2.56	14.42 ± 0.12	4	75	16.66 ± 0.01	6.19 ± 0.16	0.11	2
75679	(75679) 2000 AU97	2.80	0.22	12.56	339.4	141.9	6.2[c]	2.26	1.27	1.31	14.64 ± 0.11	4	97	17.09 ± 0.01	10.55 ± 0.12	0.19	2
77873	(77873) 2001 SQ46	2.95	0.15	6.31	155.3	83.5	6.6[c]	2.93	1.96	4.59	13.89 ± 0.10	2	38	18.02 ± 0.03	5.55 ± 0.06	0.32	2
77926	(77926) 2002 EJ140	2.53	0.24	8.70	357.8	306.5	2.6	3.00	2.01	1.83	15.96 ± 0.21	1	22	19.86 ± 0.07	5.85 ± 0.34	0.64	2
80176	(80176) 1999 UL38	2.24	0.17	5.43	321.0	80.6	1.8	2.30	1.31	2.28	15.79 ± 0.12	3	57	18.37 ± 0.03	10.79 ± 0.12	0.30	2
82943	(82943) 2001 QG117	3.06	0.13	9.90	309.5	127.7	6.4[c]	2.88	1.90	3.89	14.16 ± 0.13	4	75	18.08 ± 0.02	18.46 ± 0.36	0.36	2

Table 3
(Continued)

Obj ID	Designation	a	e	i	Ω	ω	D	$\triangle$	r	α	H_R	n	m	PTF_R	Period (hr)	$\triangle m$	U
83034	(83034) 2001 QT183	2.99	0.13	3.61	138.2	196.9	7.1	3.38	2.40	1.56	14.52 ± 0.11	4	79	19.22 ± 0.07	8.73 ± 0.23	0.36	2
83962	(83962) 2001 XW123	3.17	0.09	2.61	99.1	176.8	4.7[c]	3.44	2.46	1.58	14.76 ± 0.20	4	65	19.68 ± 0.09	5.19 ± 0.09	0.66	2
84847	(84847) 2003 AW28	3.11	0.10	12.93	120.3	299.6	6.3	2.93	1.99	6.49	14.76 ± 0.13	4	77	19.05 ± 0.06	8.28 ± 0.22	0.35	2
86474	(86474) 2000 CT79	2.80	0.04	4.06	163.9	341.9	2.9[c]	2.70	1.71	0.47	15.16 ± 0.09	2	43	18.59 ± 0.03	9.50 ± 0.19	0.21	2
90138	(90138) Diehl	2.29	0.06	0.52	218.3	124.6	1.2	2.43	1.45	2.45	16.64 ± 0.13	4	59	19.61 ± 0.08	8.07 ± 0.20	0.43	2
93000	(93000) 2000 RJ83	2.55	0.12	12.03	309.1	142.1	3.5	2.26	1.32	9.18	15.31 ± 0.14	3	65	18.26 ± 0.03	6.04 ± 0.08	0.27	2
96990	(96990) 1999 TQ215	2.69	0.21	2.99	117.2	339.4	2.5[c]	2.33	1.34	3.16	15.59 ± 0.24	4	72	18.29 ± 0.03	8.57 ± 0.08	0.71	2
97158	(97158) 1999 VV166	2.69	0.04	2.82	354.3	225.7	2.5[c]	2.70	1.80	10.50	14.98 ± 0.12	4	67	19.14 ± 0.06	5.82 ± 0.10	0.50	2
98617	(98617) 2000 WQ81	2.55	0.08	2.95	311.4	34.2	3.1	2.75	1.76	0.82	15.55 ± 0.15	4	77	19.01 ± 0.05	11.71 ± 0.29	0.46	2
A5742	(105742) 2000 SH90	3.14	0.05	21.12	301.7	340.6	8.6	3.27	2.34	6.23	14.09 ± 0.32	4	74	18.95 ± 0.05	16.27 ± 0.57	0.97	2
A6275	(106275) 2000 UY69	2.60	0.23	3.21	296.5	175.4	2.4[c]	2.00	1.04	6.83	15.21 ± 0.15	4	81	17.06 ± 0.01	19.59 ± 0.77	0.26	2
A9018	(109018) 2001 QA6	2.37	0.20	6.52	146.5	222.5	1.7	2.69	1.71	1.84	15.92 ± 0.24	4	90	19.47 ± 0.07	11.29 ± 0.26	0.71	2
A9512	(109512) 2001 QA236	2.39	0.18	5.38	141.5	345.9	5.0[c]	1.99	1.00	1.29	15.70 ± 0.21	3	44	17.36 ± 0.02	5.27 ± 0.03	0.56	2
B4122	(114122) 2002 VW49	2.29	0.18	6.11	107.7	219.3	1.4	2.66	1.72	8.44	16.36 ± 0.23	4	79	20.20 ± 0.12	5.75 ± 0.13	0.87	2
B4348[b]	(114348) 2002 XY74	2.36	0.23	3.94	299.1	108.5	3.9[c]	2.04	1.07	6.10	16.03 ± 0.29	4	78	18.18 ± 0.03	14.33 ± 0.21	0.90	2
B4561	(114561) 2003 BP52	2.40	0.18	1.00	133.9	321.3	1.5[c]	1.98	1.00	3.85	16.24 ± 0.19	4	84	18.05 ± 0.03	22.33 ± 1.46	0.58	2
B7401	(117401) 2005 AL8	2.75	0.12	9.89	110.6	31.8	4.8[c]	2.45	1.48	5.97	15.29 ± 0.08	4	77	18.56 ± 0.04	8.21 ± 0.21	0.34	2
C1192	(121192) 1999 NC22	2.57	0.13	6.90	108.1	178.0	3.3	2.90	1.93	3.88	15.43 ± 0.15	3	60	19.53 ± 0.07	11.16 ± 0.40	0.38	2
C2735	(122735) 2000 SW49	2.53	0.17	7.89	329.1	83.3	2.2	2.52	1.53	1.84	16.29 ± 0.12	4	91	19.40 ± 0.07	10.00 ± 0.43	0.32	2
C2783	(122783) 2000 SY85	2.59	0.20	3.91	105.1	300.9	1.8	2.34	1.39	8.49	16.69 ± 0.26	4	57	19.78 ± 0.10	6.23 ± 0.12	0.90	2
C8209	(128209) 2003 SS65	4.02	0.15	3.13	115.2	287.5	9.0	3.81	2.86	4.61	14.00 ± 0.21	4	69	19.56 ± 0.09	18.46 ± 1.62	0.49	2
D1048	(131048) 2000 YM38	2.62	0.06	2.83	171.0	308.5	2.3	2.48	1.50	4.56	16.24 ± 0.26	4	96	19.50 ± 0.07	11.43 ± 0.27	0.83	2
D2327	(132327) 2002 GA24	2.59	0.10	2.17	4.9	281.6	2.4	2.72	1.74	2.28	16.09 ± 0.15	1	22	19.71 ± 0.07	3.90 ± 0.24	0.52	2
D2435	(132435) 2002 GL164	2.63	0.03	3.53	104.4	50.8	2.5	2.56	1.59	4.50	16.04 ± 0.16	4	68	19.48 ± 0.08	8.28 ± 0.21	0.48	2
D5274	(135274) 2001 SH126	3.06	0.09	3.71	315.3	135.1	6.3	2.80	1.86	7.17	14.76 ± 0.11	4	74	18.82 ± 0.05	5.68 ± 0.07	0.25	2
D5316	(135316) 2001 SN277	3.08	0.14	10.17	323.3	56.1	7.3	3.31	2.32	2.01	14.46 ± 0.11	4	75	19.17 ± 0.06	6.36 ± 0.08	0.28	2
D7712	(137712) 1999 XU96	2.27	0.21	1.73	24.8	39.0	1.1	2.18	1.19	1.80	16.72 ± 0.13	4	81	19.05 ± 0.05	5.93 ± 0.07	0.48	2
D8108	(138108) 2000 DC102	2.81	0.07	17.75	147.2	55.9	3.9[c]	2.67	1.69	0.80	15.08 ± 0.16	1	18	18.46 ± 0.03	8.97 ± 1.64	0.48	2
D8503	(138503) 2000 KC58	2.36	0.15	7.90	112.3	69.5	2.0	2.15	1.21	11.13	15.52 ± 0.13	4	70	18.40 ± 0.03	6.86 ± 0.10	0.20	2
E7270	(147270) 2002 YT16	2.35	0.18	1.65	302.3	178.9	1.5[c]	1.92	0.96	9.93	16.18 ± 0.12	4	78	17.94 ± 0.02	18.46 ± 1.13	0.21	2
F1957	(151957) 2004 GE14	2.34	0.01	6.55	126.7	1.2	1.7	2.31	1.34	4.13	15.83 ± 0.14	4	65	18.82 ± 0.05	20.43 ± 1.23	0.45	2
F3672	(153672) 2001 TO189	2.43	0.12	5.63	271.6	33.4	1.6	2.72	1.75	3.34	16.04 ± 0.21	4	69	19.72 ± 0.06	28.24 ± 1.57	0.66	2
F4428	(154428) 2003 BE48	2.37	0.21	5.30	151.8	272.9	2.5[c]	2.25	1.26	1.41	16.87 ± 0.15	2	41	19.25 ± 0.06	8.14 ± 0.20	0.49	2
F5740	(155740) 2000 SF46	2.53	0.19	13.33	304.5	5.8	3.6	3.00	2.05	6.03	15.23 ± 0.19	4	75	19.52 ± 0.07	8.81 ± 0.24	0.45	2
F6926	(156926) 2003 FQ61	2.42	0.15	2.21	121.3	141.6	1.3	2.50	1.51	1.29	16.52 ± 0.29	4	80	19.61 ± 0.08	11.16 ± 0.13	0.81	2
F7770	(157770) 2007 EO57	2.33	0.17	2.12	343.1	248.0	0.9	2.16	1.17	1.86	17.30 ± 0.18	2	45	19.54 ± 0.08	9.23 ± 0.26	0.67	2
G0036	(160036) 1998 XH7	2.38	0.13	3.35	91.1	25.7	1.2	2.06	1.10	7.65	16.60 ± 0.14	2	53	18.88 ± 0.04	15.48 ± 1.77	0.45	2
G3102	(163102) 2002 AQ125	5.18	0.05	6.26	143.8	327.6	13.8	4.97	3.98	0.37	13.07 ± 0.17	4	74	19.41 ± 0.07	6.08 ± 0.04	0.54	2
G4380	(164380) 2005 EB148	2.88	0.02	3.12	136.0	1.9	5.6	2.84	1.87	4.23	15.02 ± 0.14	4	74	18.98 ± 0.05	12.47 ± 0.47	0.26	2
G7647	(167647) 2004 DW37	3.00	0.18	1.58	78.1	37.0	3.7	2.46	1.53	9.40	15.94 ± 0.29	4	58	19.42 ± 0.07	5.93 ± 0.04	0.86	2
G9134	(169134) 2001 QB36	2.99	0.14	10.75	319.2	56.3	4.8	3.08	2.19	9.11	15.36 ± 0.35	3	47	20.08 ± 0.10	10.21 ± 0.21	1.11	2
H3082	(173082) 2006 UT265	2.99	0.22	5.19	329.3	343.2	7.0[c]	3.58	2.59	0.25	15.34 ± 0.16	3	42	20.24 ± 0.11	10.21 ± 0.32	0.47	2
H5110	(175110) 2004 NF9	3.16	0.19	3.40	292.4	324.0	4.1[c]	3.23	2.24	2.13	15.37 ± 0.25	3	43	19.96 ± 0.09	7.80 ± 0.30	0.83	2
H7288[b]	(177288) 2003 XF	2.18	0.23	8.89	304.3	32.7	1.8	2.53	1.59	8.56	15.77 ± 0.16	4	66	19.52 ± 0.08	7.33 ± 0.11	0.65	2
H8014	(178014) 2006 RG	3.03	0.08	9.29	333.8	340.6	4.2[c]	3.24	2.26	1.29	14.99 ± 0.17	4	74	19.46 ± 0.08	16.27 ± 0.79	0.48	2
I9772	(189772) 2002 CQ78	5.14	0.02	8.17	343.6	115.3	15.2	5.08	4.09	0.97	12.85 ± 0.23	4	65	19.51 ± 0.08	5.96 ± 0.04	0.70	2
J0620	(190620) 2000 WC39	2.58	0.26	5.05	154.1	225.2	2.1	2.86	1.88	2.96	16.38 ± 0.20	3	46	20.22 ± 0.12	6.19 ± 0.08	0.69	2
J4968	(194968) 2002 AQ178	2.53	0.13	1.68	86.3	66.2	3.7[c]	2.25	1.33	11.00	16.29 ± 0.27	4	74	19.36 ± 0.07	10.55 ± 0.12	0.84	2

Table 3
(Continued)

Obj ID	Designation	a	e	i	Ω	ω	D	$\triangle$	r	α	H_R	n	m	PTF$_R$	Period (hr)	$\triangle m$	U
J7166	(197166) 2003 UG277	2.77	0.05	2.97	270.5	223.6	2.3	2.65	1.67	2.89	16.16 ± 0.17	3	54	19.75 ± 0.09	7.93 ± 0.31	0.54	2
J8675	(198675) 2005 CY2	2.74	0.18	4.43	126.7	306.5	2.4	2.34	1.38	6.56	16.10 ± 0.14	4	69	19.31 ± 0.07	12.97 ± 0.55	0.40	2
K0296	(200296) 2000 AV218	2.78	0.11	2.76	312.6	98.5	4.5[c]	2.65	1.72	8.38	16.02 ± 0.24	4	54	20.02 ± 0.11	5.33 ± 0.06	0.77	2
K04X75P	2004 XP75	2.68	0.29	2.07	309.3	126.5	1.8	2.26	1.27	3.49	16.76 ± 0.18	4	81	19.26 ± 0.06	16.55 ± 0.59	0.45	2
K09W25J	2009 WJ25	2.56	0.34	28.77	300.6	86.5	1.9	2.28	1.34	8.72	16.58 ± 0.24	4	80	19.56 ± 0.08	11.71 ± 0.29	0.80	2
K09X12N	2009 XN12	2.40	0.16	1.85	298.3	119.6	1.7[c]	2.14	1.17	5.56	17.59 ± 0.25	4	52	20.02 ± 0.12	6.44 ± 0.09	0.86	2
K6638	(206638) 2003 WA190	2.78	0.20	14.63	337.6	66.9	4.5[c]	2.86	1.87	0.55	15.84 ± 0.15	2	44	19.61 ± 0.08	5.19 ± 0.08	0.47	2
L1435	(211435) 2002 YM9	3.04	0.31	2.05	241.6	154.9	4.1	3.03	2.06	4.35	15.69 ± 0.24	4	61	19.96 ± 0.09	8.81 ± 0.08	0.69	2
L4843	(214843) 2006 VO170	3.25	0.11	1.21	171.4	88.5	4.7	3.35	2.37	2.43	15.39 ± 0.26	4	46	20.18 ± 0.11	7.56 ± 0.12	0.95	2
L7232	(217232) 2003 BU48	2.38	0.16	1.60	321.7	177.0	1.1	2.00	1.01	2.69	16.87 ± 0.12	4	79	18.67 ± 0.04	8.89 ± 0.17	0.25	2
M5445	(225445) 2000 DO36	2.32	0.16	2.15	349.1	192.9	0.8	2.11	1.16	8.98	17.61 ± 0.14	4	53	20.14 ± 0.13	4.12 ± 0.07	0.45	2
N0067	(230067) 2000 TG72	2.58	0.18	5.44	100.4	319.5	1.8	2.30	1.38	11.34	16.69 ± 0.15	2	50	19.84 ± 0.09	9.32 ± 0.48	0.44	2
N5885	(235885) 2005 CK10	2.71	0.11	12.55	344.3	358.5	2.8	3.01	2.03	1.67	15.78 ± 0.23	4	74	19.89 ± 0.11	6.53 ± 0.09	0.79	2
N6497	(236497) 2006 GU20	2.61	0.11	3.50	129.9	340.1	1.7	2.39	1.40	1.99	16.89 ± 0.21	4	72	19.78 ± 0.10	8.14 ± 0.14	0.65	2
O1827	(241827) 2001 SR209	3.12	0.19	1.74	69.7	348.2	3.8	2.76	1.81	6.54	15.85 ± 0.22	4	62	19.79 ± 0.09	7.56 ± 0.18	0.75	2
O2897	(242897) 2006 KH73	2.68	0.06	8.94	140.4	4.5	3.1[c]	2.52	1.53	1.49	16.07 ± 0.19	4	81	19.19 ± 0.06	30.97 ± 3.32	0.64	2
Q8265	(268265) 2005 OF5	2.22	0.18	4.53	154.5	145.8	1.0	2.53	1.55	1.08	17.08 ± 0.20	4	64	20.15 ± 0.11	7.06 ± 0.11	0.69	2
R5911	(275911) 2001 TD149	2.45	0.20	3.51	96.9	287.9	1.3	2.37	1.42	7.22	16.53 ± 0.29	3	29	19.83 ± 0.10	5.68 ± 0.10	0.79	2
S2694	(282694) 2006 AO5	1.90	0.08	19.11	332.5	49.6	1.0	2.00	1.01	1.12	16.98 ± 0.11	3	57	18.74 ± 0.04	11.85 ± 0.29	0.21	2
S5409	(285409) 1999 UF32	2.67	0.12	2.11	53.4	79.6	1.5	2.36	1.37	2.18	17.10 ± 0.29	3	46	20.04 ± 0.12	6.67 ± 0.19	0.82	2
X1570	(331570) 2001 QS67	2.40	0.18	7.75	303.7	53.8	1.4	2.52	1.55	4.75	16.30 ± 0.25	4	45	19.67 ± 0.08	5.55 ± 0.06	0.63	2
Y3133	(343133) 2009 FY1	3.04	0.09	12.32	108.9	356.7	3.6	2.76	1.81	6.43	15.96 ± 0.23	4	61	19.94 ± 0.09	11.16 ± 0.27	0.79	2
Y7295	(347295) 2011 OM3	3.17	0.10	15.76	298.3	33.0	4.8	3.41	2.45	4.13	15.37 ± 0.13	4	57	20.40 ± 0.13	10.32 ± 0.32	0.41	2
b3533	(373533) 2001 TF11	2.44	0.19	1.52	286.2	77.3	1.1	2.53	1.57	5.22	16.86 ± 0.18	4	61	20.20 ± 0.11	7.27 ± 0.17	0.61	2
c6924	(386924) 2011 KV28	2.30	0.17	7.45	152.0	92.7	0.8	2.29	1.32	5.37	17.46 ± 0.16	4	52	20.28 ± 0.12	6.00 ± 0.15	0.49	2

Note. The amplitudes of the objects with partial light-curve coverage and light curves with a single minimum should be treated as lower limits. Also, see the note and footnotes associated with Table 2 for nomenclature and explanation.

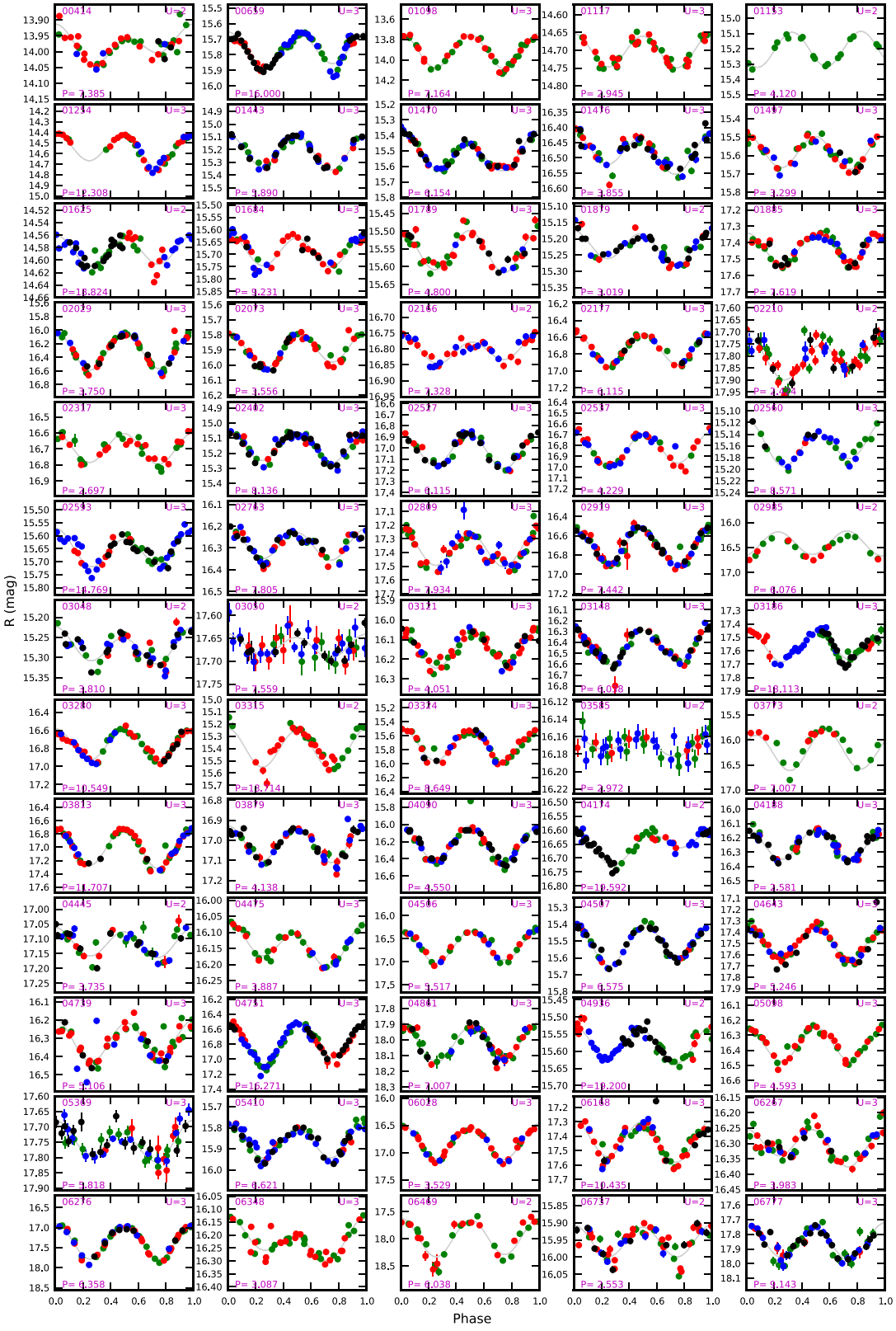

Figure 4. Set of 65 folded light curves for the PTF-U2 asteroids. The green, red, blue, and black circles represent observations taken on different nights. The asteroid designation is given in each plot along with its derived rotation period P in hours and quality code U.

(An extended version of this figure is available.)

Table 4
Bright Asteroids with Large Light-curve Variation and without Rotation-period Determination

Obj ID	Designation	a	e	i	Ω	ω	D	$\triangle$	r	α	H_R	n	m	PTF_R	$\triangle m$
02979	(2979) Murmansk	3.12	0.16	11.42	148.5	197.2	18.5[a]	3.60	2.62	1.55	12.35 ± 0.18	4	83	17.41 ± 0.02	0.60
03427	(3427) Szentmartoni	2.28	0.13	2.60	310.1	76.4	5.0[a]	2.43	1.44	1.01	13.69 ± 0.24	4	84	16.55 ± 0.01	0.75
04251	(4251) Kavasch	2.41	0.18	3.34	115.4	132.6	4.3[a]	2.67	1.69	2.77	13.62 ± 0.17	4	69	17.20 ± 0.01	0.66
04869	(4869) Piotrovsky	2.24	0.17	3.55	96.3	217.6	6.5[a]	2.60	1.64	6.01	12.93 ± 0.32	4	78	16.57 ± 0.01	0.83
05827	(5827) Letunov	2.19	0.13	3.70	105.4	284.0	5.0	2.16	1.25	12.32	13.53 ± 0.32	4	74	16.38 ± 0.01	0.97
07321	(7321) 1979 MZ2	2.53	0.09	2.29	154.5	328.0	5.2[a]	2.34	1.35	3.20	13.72 ± 0.22	4	83	16.44 ± 0.01	0.80
08475	(8475) Vsevoivanov	3.08	0.25	4.83	118.5	266.1	14.3[a]	2.85	1.87	2.59	12.92 ± 0.25	4	79	16.75 ± 0.01	0.64
09319	(9319) 1988 RV11	2.25	0.15	2.94	165.5	97.5	5.5[a]	2.32	1.33	1.02	14.87 ± 0.18	4	85	17.53 ± 0.02	0.66
10224	(10224) Hisashi	2.43	0.17	3.43	126.4	188.1	8.5[a]	2.82	1.87	6.49	14.19 ± 0.26	2	26	18.43 ± 0.04	0.64
10252	(10252) Heidigraf	2.85	0.07	2.26	33.3	290.1	5.8[a]	3.05	2.06	1.44	13.16 ± 0.19	4	86	17.25 ± 0.01	0.56
10943	(10943) Brunier	2.15	0.17	0.75	268.0	74.1	2.6	2.38	1.42	7.36	14.91 ± 0.28	4	74	18.08 ± 0.03	0.97
13468	(13468) 3378 T-3	2.32	0.16	0.88	138.1	8.5	2.4[a]	1.98	1.03	9.07	14.83 ± 0.21	3	72	17.07 ± 0.01	0.58
15626	(15626) 2000 HR50	3.95	0.11	1.80	138.0	289.7	18.5	3.85	2.86	0.74	12.43 ± 0.22	4	85	17.70 ± 0.02	0.64
18721	(18721) 1998 HC146	3.21	0.05	7.22	106.0	149.2	11.2[a]	3.32	2.39	6.40	13.59 ± 0.22	4	72	18.54 ± 0.04	0.56
18797	(18797) 1999 JT64	2.59	0.23	4.21	106.9	234.8	5.0	2.93	1.96	4.44	14.53 ± 0.16	4	75	18.83 ± 0.05	0.52
19178	(19178) Walterbothe	2.58	0.26	3.89	276.3	11.4	6.1	3.24	2.26	3.17	14.09 ± 0.26	4	78	18.90 ± 0.05	0.82
22034	(22034) 1999 XL168	2.68	0.06	6.79	331.6	196.4	4.8[a]	2.51	1.53	0.79	13.50 ± 0.20	4	84	16.34 ± 0.01	0.67
22904	(22904) 1999 TL19	2.62	0.09	4.78	173.4	133.8	6.7[a]	2.83	1.85	2.60	14.45 ± 0.07	1	21	18.24 ± 0.02	0.51
22973	(22973) 1999 VW16	2.70	0.11	1.93	288.5	89.3	3.9[a]	2.70	1.73	4.02	14.54 ± 0.27	4	76	18.30 ± 0.04	0.85
23757	(23757) Jonmunoz	2.28	0.14	7.05	116.4	245.2	2.3[a]	2.40	1.48	9.97	14.56 ± 0.15	4	73	17.86 ± 0.02	0.51
24527	(24527) 2001 CA6	2.19	0.13	6.90	335.4	34.7	2.1	2.40	1.41	0.48	15.39 ± 0.26	3	64	18.12 ± 0.03	0.75
25349	(25349) 1999 RL127	2.65	0.14	11.58	295.7	152.2	5.6[a]	2.32	1.35	5.45	13.58 ± 0.20	4	78	16.22 ± 0.01	0.62
29074	(29074) 5160 T-3	2.86	0.23	13.96	156.5	133.8	4.2[a]	3.26	2.27	0.53	14.02 ± 0.13	4	77	18.49 ± 0.04	0.64
30025	(30025) 2000 DJ26	2.30	0.17	5.53	150.0	138.4	2.0	2.51	1.53	2.23	15.53 ± 0.22	4	81	18.67 ± 0.04	0.58
32868	(32868) 1993 FM25	3.07	0.13	1.50	241.9	270.2	5.6[a]	2.66	1.69	5.25	14.47 ± 0.34	4	74	18.12 ± 0.03	1.04
35501	(35501) 1998 FM41	2.56	0.14	0.76	254.2	200.0	2.6[a]	2.23	1.27	7.53	15.21 ± 0.18	4	80	17.92 ± 0.02	0.51
36402	(36402) 2000 OT47	2.54	0.16	2.73	119.2	237.4	5.0	2.72	1.78	7.61	14.53 ± 0.29	2	24	18.68 ± 0.06	0.67
37445	(37445) 3056 P-L	2.40	0.13	7.20	295.6	317.5	2.8	2.61	1.65	6.26	14.77 ± 0.14	2	33	18.34 ± 0.04	0.79
38222	(38222) 1999 NP31	2.59	0.12	3.50	101.5	212.3	4.5	2.89	1.94	6.06	14.72 ± 0.20	4	80	18.99 ± 0.05	0.50
39574	(39574) 1993 FM5	2.66	0.11	2.20	104.1	297.3	6.2[a]	2.55	1.59	5.77	14.97 ± 0.35	4	76	18.44 ± 0.04	0.97
40287	(40287) 1999 JS61	2.13	0.04	0.33	189.6	133.6	1.9	2.21	1.22	0.33	15.66 ± 0.23	2	45	17.92 ± 0.02	0.62
41967	(41967) 2000 XE39	2.59	0.18	12.33	326.0	73.3	3.5	2.66	1.68	2.65	15.31 ± 0.20	4	61	18.81 ± 0.05	0.55
42297	(42297) 2001 UL73	3.16	0.17	1.52	137.1	354.8	6.5	2.62	1.66	5.52	14.71 ± 0.22	3	60	18.31 ± 0.03	0.76
45610	(45610) 2000 DJ48	2.86	0.11	1.50	352.9	14.3	7.5	2.94	1.98	5.43	14.38 ± 0.13	4	73	18.62 ± 0.05	0.52
45904	(45904) 2000 YV29	2.68	0.13	13.31	116.9	340.2	4.2[a]	2.37	1.45	10.83	13.75 ± 0.21	4	76	17.06 ± 0.01	0.64
46714	(46714) 1997 HF7	2.33	0.18	1.46	54.7	10.2	2.1[a]	2.02	1.06	7.80	15.07 ± 0.17	4	62	17.23 ± 0.01	0.51
49589	(49589) 1999 CQ149	2.95	0.09	2.05	171.4	315.7	6.0	2.72	1.73	0.75	14.86 ± 0.21	4	77	18.34 ± 0.04	0.69
50886	(50886) 2000 GW39	2.97	0.13	0.82	65.1	276.7	6.4[a]	3.18	2.20	1.69	14.57 ± 0.24	3	26	18.87 ± 0.08	0.64
51202	(51202) 2000 JR6	2.97	0.12	13.70	119.2	296.7	7.5[a]	2.75	1.77	2.87	13.76 ± 0.12	4	82	17.69 ± 0.02	0.52
54158	(54158) 2000 HY48	2.37	0.12	2.24	66.2	108.3	1.5	2.19	1.23	7.59	16.14 ± 0.23	2	45	18.80 ± 0.05	0.85
54587	(54587) 2000 QM189	3.13	0.04	11.17	110.3	157.7	4.4[a]	3.23	2.29	6.44	14.13 ± 0.20	3	43	18.85 ± 0.04	0.51
55652	(55652) 4048 P-L	2.98	0.08	2.44	217.8	139.3	6.9[a]	3.19	2.20	1.93	14.21 ± 0.18	4	73	18.68 ± 0.04	0.57
56702	(56702) 2000 LQ28	3.14	0.25	15.78	313.6	37.0	12.1[a]	3.79	2.82	3.59	13.07 ± 0.26	3	60	18.56 ± 0.04	1.15
57175	(57175) 2001 QD24	2.44	0.21	3.09	111.9	287.7	1.9[a]	2.21	1.23	4.45	15.67 ± 0.27	2	24	18.33 ± 0.05	0.54
59263	(59263) 1999 CK30	2.43	0.19	2.25	100.6	301.1	1.9	2.24	1.30	8.96	15.64 ± 0.25	4	69	18.54 ± 0.04	0.69
59812	(59812) 1999 RA18	3.24	0.04	14.94	343.7	225.0	11.9[a]	3.17	2.18	1.37	13.53 ± 0.17	4	88	17.93 ± 0.03	0.62
61480	(61480) 2000 QY39	3.04	0.09	9.89	328.4	322.6	8.1	3.23	2.24	0.74	14.21 ± 0.17	4	76	18.65 ± 0.04	0.57
62043	(62043) 2000 RH65	3.23	0.10	8.72	170.3	248.1	9.6[a]	3.18	2.20	3.61	13.78 ± 0.22	2	34	18.42 ± 0.05	0.81
64387	(64387) 2001 UW144	2.38	0.15	2.40	91.5	145.4	1.9	2.28	1.29	1.88	15.64 ± 0.23	3	64	18.09 ± 0.02	0.55
67917	(67917) 2000 WU109	2.52	0.15	4.37	317.0	327.4	2.4[a]	2.76	1.77	0.93	14.91 ± 0.25	2	34	18.70 ± 0.06	0.98
69727	(69727) 1998 HD145	2.57	0.12	8.10	140.5	125.1	2.5[a]	2.66	1.67	1.45	15.21 ± 0.23	2	40	18.51 ± 0.05	0.61

Table 4
(Continued)

Obj ID	Designation	a	e	i	Ω	ω	D	$\triangle$	r	α	H_R	n	m	PTF_R	$\triangle m$
70615	(70615) 1999 TZ204	2.71	0.06	2.75	302.8	164.3	3.0[a]	2.56	1.58	3.29	14.99 ± 0.26	4	82	18.29 ± 0.03	0.86
75653	(75653) 2000 AG64	2.33	0.04	9.38	122.1	129.5	5.2[a]	2.40	1.42	3.60	14.52 ± 0.25	1	14	17.48 ± 0.02	0.85
77831	(77831) 2001 QL226	3.00	0.07	7.73	310.4	178.5	9.2	2.79	1.81	3.54	13.93 ± 0.11	4	81	17.72 ± 0.02	0.56
78479	(78479) 2002 RO52	2.84	0.07	3.07	128.4	240.1	3.5[a]	3.00	2.01	1.00	14.71 ± 0.19	1	19	18.71 ± 0.05	0.66
80448	(80448) 1999 YA17	2.31	0.11	9.72	293.9	99.1	4.1[a]	2.25	1.28	5.19	15.31 ± 0.20	3	51	18.04 ± 0.04	0.65
80451	(80451) Alwoods	2.29	0.09	5.70	114.6	351.1	1.6	2.09	1.16	11.18	15.96 ± 0.17	4	72	18.54 ± 0.04	0.52
81985	(81985) 2000 QV122	3.01	0.23	7.82	333.5	292.2	5.4[a]	3.13	2.14	0.38	13.89 ± 0.20	4	86	18.01 ± 0.02	0.59
83524	(83524) 2001 ST148	2.98	0.10	8.28	332.6	4.2	4.5[a]	3.26	2.27	0.79	14.23 ± 0.15	4	83	18.62 ± 0.04	0.58
84852	(84852) 2003 AN38	3.06	0.08	9.79	144.5	71.1	7.6[a]	2.95	1.96	1.40	14.97 ± 0.21	2	34	18.96 ± 0.05	0.52
88367	(88367) 2001 PY8	2.39	0.12	5.80	296.4	32.5	2.0	2.63	1.66	5.01	15.50 ± 0.28	2	20	18.97 ± 0.06	0.55
90232	(90232) 2003 BD27	3.12	0.19	17.62	155.4	334.3	7.8[a]	2.55	1.57	2.69	14.59 ± 0.29	4	78	17.87 ± 0.02	0.83
90997	(90997) 1998 BC	2.49	0.04	8.05	329.1	263.4	3.8[a]	2.47	1.48	0.64	15.04 ± 0.27	4	88	17.89 ± 0.02	0.93
93114	(93114) 2000 SE58	2.52	0.07	1.95	189.0	246.0	2.9	2.45	1.47	2.74	15.70 ± 0.26	4	66	18.75 ± 0.04	0.84
98404	(98404) 2000 UT8	2.56	0.21	0.36	36.0	1.5	3.4[a]	2.72	1.73	2.10	15.29 ± 0.17	2	33	18.79 ± 0.07	0.54
A4108	(104108) 2000 EH45	2.91	0.03	1.38	244.2	15.2	3.1[a]	2.98	2.01	2.52	14.94 ± 0.16	4	76	18.91 ± 0.06	0.54
A8184	(108184) 2001 HH15	2.24	0.22	5.05	342.7	313.4	3.3[a]	2.57	1.58	0.51	15.61 ± 0.31	1	22	18.71 ± 0.07	1.36
B5812	(115812) 2003 UD243	2.75	0.11	2.71	96.9	346.3	3.2	2.63	1.64	2.37	15.50 ± 0.13	1	20	18.93 ± 0.07	0.63
C5001	(125001) 2001 TG154	2.42	0.10	6.76	105.8	290.3	1.8	2.35	1.37	3.64	15.77 ± 0.19	2	24	18.55 ± 0.05	0.50
C6117	(126117) 2001 YW113	2.54	0.17	12.67	293.2	140.1	2.8[a]	2.20	1.24	7.25	15.81 ± 0.38	4	74	18.51 ± 0.04	1.15
C6488	(126488) 2002 CD55	2.53	0.14	3.74	317.3	285.2	3.5	2.48	1.49	0.85	15.26 ± 0.16	4	69	18.37 ± 0.04	0.88
C7599	(127599) 2003 BE18	2.40	0.19	0.37	65.1	354.1	1.4[a]	2.08	1.11	6.48	15.97 ± 0.18	4	75	18.27 ± 0.04	0.89
D0982	(130982) 2000 WH130	2.63	0.16	3.21	77.4	29.8	4.1[a]	2.21	1.26	8.60	16.04 ± 0.43	3	52	18.82 ± 0.05	1.05
D5405	(135405) 2001 TF226	3.08	0.23	16.85	150.9	258.2	6.5[a]	3.11	2.12	0.59	14.65 ± 0.21	2	26	18.86 ± 0.05	0.66
E4543	(144543) 2004 EV94	3.01	0.08	15.72	150.5	90.3	6.1	2.97	1.98	1.43	14.84 ± 0.32	3	60	18.89 ± 0.05	0.84
E7041	(147041) 2002 RE65	2.33	0.26	4.83	105.9	256.5	1.6[a]	2.40	1.42	3.56	15.27 ± 0.27	2	23	18.46 ± 0.05	0.61
E7448	(147448) 2003 YT136	2.24	0.07	8.11	119.5	328.3	1.2	2.09	1.11	4.94	16.58 ± 0.15	4	69	18.80 ± 0.05	0.51
F6799	(156799) 2003 BD18	2.37	0.17	0.81	149.1	284.6	1.2	2.23	1.24	1.14	16.59 ± 0.20	4	80	18.98 ± 0.05	0.84
F7530	(157530) 2005 TX17	2.41	0.15	3.03	141.5	286.5	1.6[a]	2.13	1.15	5.06	16.41 ± 0.18	3	51	18.74 ± 0.05	0.55
G1236	(161236) 2003 AK29	2.36	0.14	3.21	294.4	199.8	1.2	2.04	1.05	4.24	16.58 ± 0.22	4	72	18.54 ± 0.03	0.62
G3890	(163890) 2003 SC199	2.77	0.07	4.39	297.4	92.1	4.6[a]	2.74	1.77	4.16	15.24 ± 0.16	4	72	18.90 ± 0.05	0.63
H1914	(171914) 2001 SM75	3.12	0.20	4.49	306.0	112.5	7.9	2.94	1.97	4.45	14.29 ± 0.13	2	28	18.48 ± 0.04	0.68
I3712	(183712) 2003 YY61	2.22	0.16	4.94	105.7	299.2	1.2	2.05	1.08	6.18	16.62 ± 0.14	4	69	18.80 ± 0.05	0.57
J0951	(190951) 2001 VU62	2.44	0.13	2.64	332.4	122.6	1.7[a]	2.23	1.25	1.61	15.53 ± 0.20	2	37	17.83 ± 0.03	1.05
J0991	(190991) 2001 XQ238	2.47	0.15	1.90	6.1	81.8	1.9	2.29	1.30	1.25	15.60 ± 0.16	1	22	18.16 ± 0.02	0.53
J3212	(193212) 2000 QE224	2.56	0.29	10.47	337.7	90.6	3.1[a]	2.31	1.33	2.39	16.11 ± 0.14	2	33	18.77 ± 0.06	0.54
J3656	(193656) 2001 DK45	2.69	0.14	1.77	346.9	156.0	3.8[a]	2.34	1.38	6.91	15.85 ± 0.22	4	77	18.99 ± 0.06	0.63
J5207	(195207) 2002 DN2	2.56	0.13	30.58	115.0	340.3	4.1[a]	2.24	1.27	5.21	15.02 ± 0.18	4	83	17.55 ± 0.02	0.50
J7712	(197712) 2004 PS3	2.37	0.09	6.12	332.9	273.5	1.6	2.36	1.37	0.82	15.96 ± 0.16	2	47	18.69 ± 0.04	0.86
K9327	(209327) 2004 BC92	2.92	0.22	4.49	164.6	354.0	4.0	2.29	1.31	2.92	15.74 ± 0.15	4	77	18.39 ± 0.03	0.51
L6446	(216446) 2009 FA45	3.05	0.14	12.84	147.6	307.0	5.2	2.78	1.79	1.73	15.18 ± 0.16	2	42	18.84 ± 0.04	0.51
L7813	(217813) 2001 BD19	2.18	0.09	5.77	324.4	114.0	1.2	2.10	1.11	0.84	16.67 ± 0.33	3	35	18.66 ± 0.05	1.01
M0448	(220448) 2003 YF65	2.23	0.15	5.11	105.5	312.7	1.3	2.03	1.11	12.60	16.52 ± 0.17	4	90	18.80 ± 0.04	0.57
M2177	(222177) 2000 BL29	2.30	0.19	6.23	332.3	114.4	1.2[a]	2.06	1.07	0.84	16.93 ± 0.14	4	83	18.73 ± 0.04	0.58
Y2031	(342031) 2008 RA108	2.59	0.16	14.12	332.9	72.2	3.1	2.64	1.65	0.97	15.54 ± 0.30	4	55	18.81 ± 0.07	1.52
c2447	(382447) 2000 DZ36	2.79	0.24	9.05	340.2	133.0	2.1	2.24	1.25	2.77	16.39 ± 0.15	4	77	18.86 ± 0.06	1.09

Note. Δm is the light-curve variation over our four-night observing time. Also, see the note and footnotes associated with Table 2 for the nomenclature and explanation.

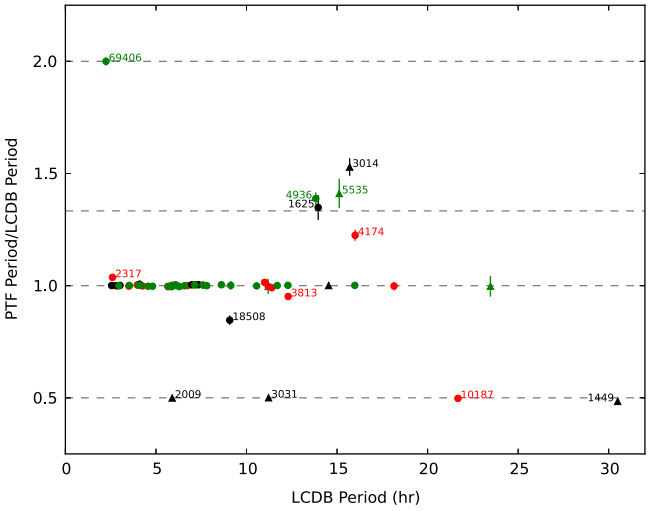

Figure 5. Comparison of 53 derived rotation periods for PTF-U2s with matching objects in the LCDB. Filled circles and filled triangles correspond to asteroids with full and partial rotational-phase coverages, respectively. Red, green, and black indicate that the U of the PTF-U2 is $>$, $=$, or $<U$ of the matching LCDB object, respectively.

the orbital elements and observational conditions, are summarized in Table 2, and their folded light curves are provided in Figures 4(a)–(u).

In addition, there are 169 objects that have folded light curves with only partial coverage in rotational phase, but nevertheless demonstrate a clear trend (hereafter, PTF-Ps). Most PTF-Ps seem to be long-period objects (i.e., $f < 2$ rev day^{-1}), and therefore we only can obtain their partial light curves. We estimated a lower limit on the amplitude based on the light-curve variation and their actual rotation period should be longer than that derived. These objects are summarized in Table 3 and their folded light curves are given in Figures 4 (v)–(x).

We also found 63 asteroids showing large amplitudes and deep V-shaped minima in their light curves (see Figure 4(y)). Most of them are probably contact binaries or very elongate asteroids that have smooth transitions from minimum to maximum (see 3169 Ostro as an example in Descamps et al. 2007). Among these, we use the typical light curve features for binary asteroids, i.e., a deep V-shaped minimum with a "shoulder" due to the abrupt drop in brightness at the onset of eclipse/occultation and an inverse U-shaped maxima (Behrend et al. 2006), to identify several binary asteroid candidates, that is, 51495 and 56005, and maybe 46165 and B4348. These candidates need to be confirmed through follow-up observations. Moreover, the asynchronous binary candidate (69406) 1995 SX48 (Warner 2014) was also observed in our survey, and we detected a primary rotation period of ~4.49 hr from our relatively scattered light curve.

Among the 1438 PTF-U2s, 65 objects have published rotation periods in the asteroid Light Curve Database (LCDB; Warner et al. 2009).[8] To ensure the reliability of our period analysis, we compared the rotation periods between our survey data and those of matching objects in the LCDB, and we show the results in Figure 5. Most of the matches have consistent derived rotation periods. However, there are 13 outliers. Despite the 6 PTF-Ps (1449, 2009, 3014, 3031, 5450, and 5535) that are relatively uncertain in our determination of rotation periods and the 4 (2317, 3813, 4174, and 10187) that have better quality codes in our results than in the LCDB, there are still 3 outliers (1625, 4936, and 185086) that have rotation periods which are significantly different from the rotation period of their LCDB counterpart within a reasonable uncertainty. The possible reasons behind this are discussed below.

Asteroid 1625 has a long rotation period of 13.96 hr with $U = 3$ (Higgins 2011). We were only able to obtain part of its full light curve, and thus derived a rotation period of 18.82 hr, which is ~4/3 of the corresponding LCDB rotation period (see Figure 12(a)).

Asteroid 4936 has $U = 2$ ratings from both our determination and the LCDB. When the PTF light curve is folded with the rotation period of 13.83 hr listed in the LCDB, it does not give a clear trend. However, folding the PTF light curve with a rotation period of 19.2 hr gives a much better result, one that looks better, in fact, than the similarly folded light curve for this asteroid reported by Pray et al. (2008). Therefore, we believe our rotation period is more accurate than the LCDB rotation period.

Asteroid 185086 also has a long rotation period of 9.08 hr with $U = 3$ (Masiero et al. 2009). It is also a faint object (see Figure 4(o)), which is one possible reason why we were only able to obtain a sparse light curve, and therefore make a less accurate determination of its rotation period.

Among the 6551 PTF-detected asteroids, 96 objects have $R < 19$ mag (i.e., large) and $\Delta m > 0.5$ mag, but do not have a rotation-period determination. These asteroids are listed in Table 4. The associated light curves show a long-trend variation over our four-night observing time, suggesting that they very likely have a spin rate of <1 rev day^{-1}. In order to obtain their relatively long rotation periods, observations with a longer time baseline are required, which is beyond the capabilies of our present survey strategy. Thus, we cannot more accurately determine the spin rates of these large, long-period asteroids.

4.2. Detecting Simulation for Asteroid Rotation Period

We adopted an approach similar to that described in Masiero et al. (2009) to carry out the detecting simulation for asteroid rotation period. The apparent magnitude (m) distribution of PTF-detected asteroids can be described as

$$N = \frac{2.5^{(M-12)}}{1 + e^{(M-20.5)/0.25}}. \quad (3)$$

This function accounts for the number increase and falloff along with apparent magnitude in a magnitude-limited survey (Jedicke & Herron 1997). Instead of using a sophisticated asteroid shape to construct a synthetic light curve that introduces formidable time-consuming computation, the synthetic objects were assumed to be relaxed triaxial ellipsoids having equal axes in b and c, rotating around the principle-axis a. Therefore, the light curves can be written as

$$m = 2.5 \log_{10} \sqrt{1 + \left[\left(\frac{b}{a}\right)^2 - 1\right] \cos^2(2\pi\phi) \sin^2\theta}, \quad (4)$$

[8] http://www.minorplanet.info/lightcurvedatabase.html

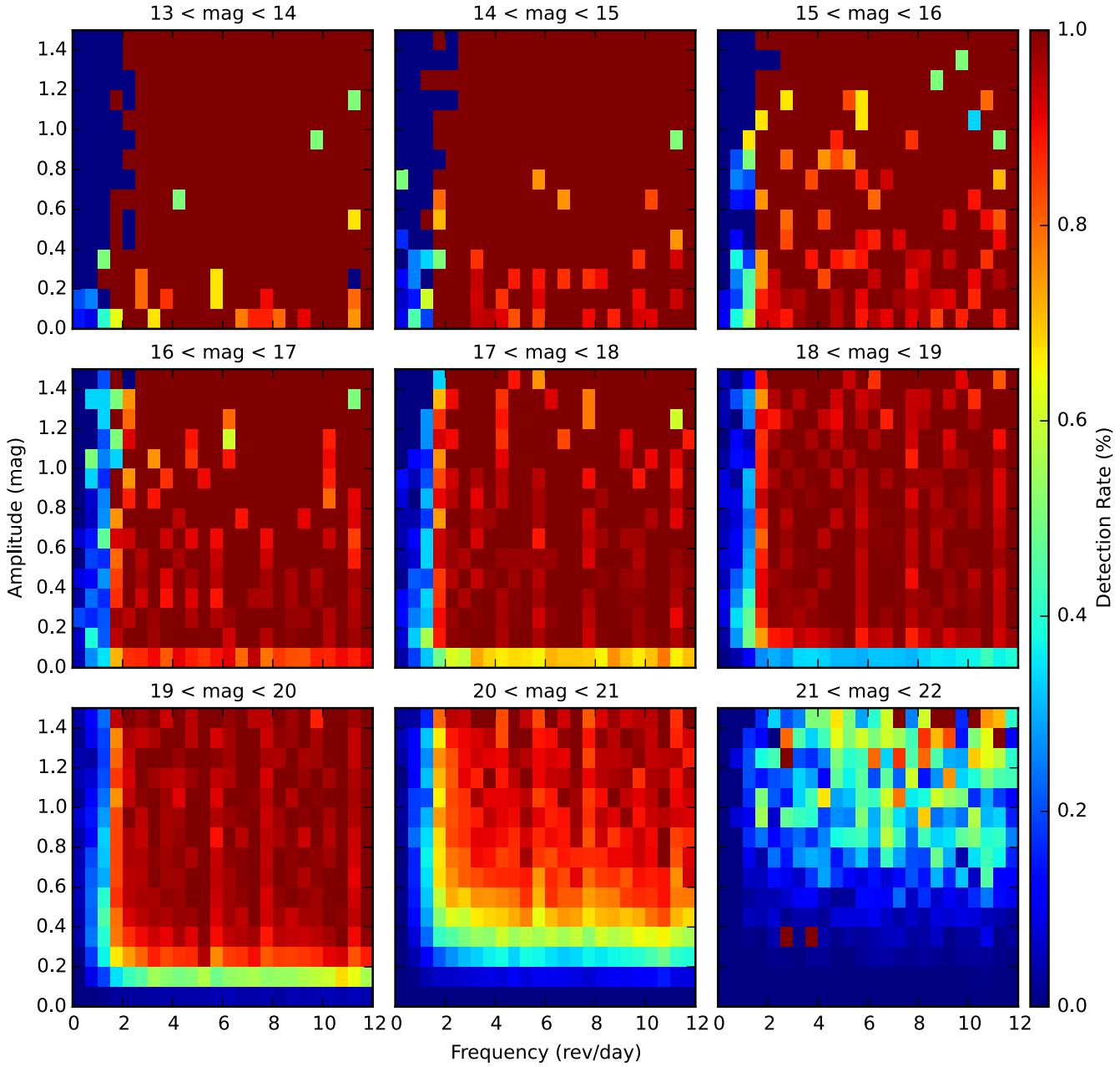

Figure 6. Detection rates for asteroid rotation period. The color bar scale on the right shows the percentage of successful recovery for the rotation period of synthetic objects. The apparent magnitude interval is indicated at the top of each plot.

and the amplitude (Δm) can be written as

$$\Delta m = 2.5 \log_{10}\left[\cos^2\theta + \left(\frac{b}{a}\right)^2 \sin^2\theta\right]^{-1/2}, \quad (5)$$

where ϕ is the rotational phase and θ is the angle between the line of sight and the spin vector (Lacerda & Luu 2003; Lacerda & Jewitt 2007). The cadences of the synthetic light curves were chosen to be identical to the survey observations, and the numbers of synthetic measurements were assigned according to the number of detections of PTF-detected asteroids with different apparent magnitudes.

We generated 402,000 synthetic light curves that uniformly distribute with a frequency of $0 \leqslant f \leqslant 12$ rev day^{-1}, a pole orientation of $10 \leqslant \theta \leqslant 90$ degree, and an axis ratio of $0.1 \leqslant b/a \leqslant 1$. Then, these synthetic light curves were analyzed by the aforementioned second-order Fourier series method to search for assigned periods. We defined a successful period determination as (a) the derived period is within 5% of the original period, (b) the folded light curve of the derived period has double peaks or double dips, and (c) the assigned photometric error is smaller than the derived amplitude. Therefore, the "PTF-P"-like objects could not be picked up in the simulation.

Figure 6 shows the detection rate *of f* versus Δm for various apparent magnitude intervals. In general, the detecting efficiency increases with Δm and decreases with m. Moreover, the detection rate becomes very low for long-period objects in which we see an obvious drop off at $f < 1.5$ rev day^{-1}. When

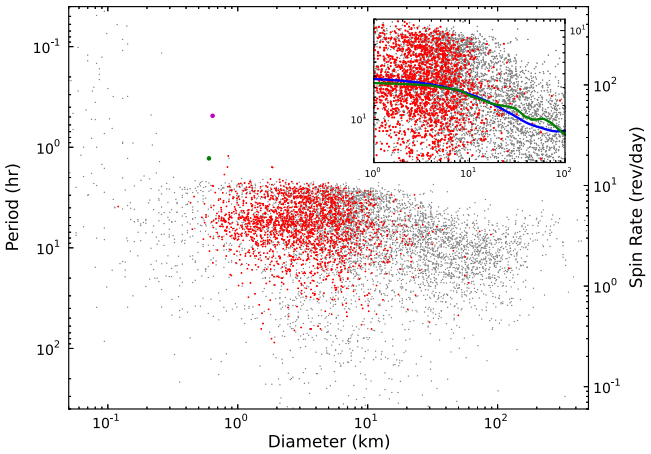

Figure 7. Asteroid rotation period vs. diameter. The red and gray filled circles are PTF-U2s and LCDB objects of $U \geqslant 2$, respectively. The SFRs 2001 OE84 (magenta) and 2005 UW163 (green) are indicated with large filled circles. The inset plot is a zoom-in of the dense region, where the green and blue lines are the regressions of the spin rates for PTF-U2s and LCDB objects computed using LOWESS, respectively.

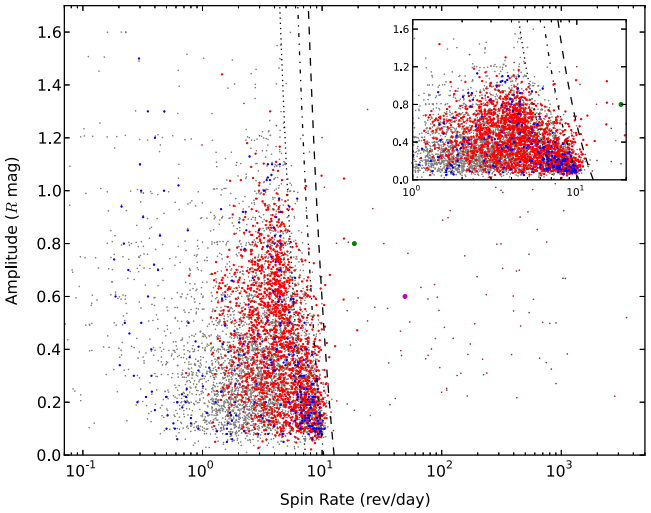

Figure 8. Light-curve amplitude vs. spin rate. The red, gray, blue, and brown filled circles are PTF-U2s, LCDB of $D \geqslant 0.2$ km, P08 (update 2014 April 20), and LCDB of $D < 0.2$ km, respectively. The dashed, dot–dashed, and dotted lines represent the spin-rate limits for rubble-pile asteroids with bulk densities of 3, 2, and 1 g cm^{-3} (Pravec & Harris 2000), respectively. The inset plot is a zoom-in of $1 < f < 12$ rev day^{-1}.

the assigned photometric error is comparable to Δm for a synthetic object, the simulation would not be able to detect its rotation period. Therefore, the chance of detecting small-amplitude objects becomes much lower for faint objects. However, we do not see any favoring of detecting particular frequency with fixed light-curve amplitude except for long-period objects (i.e., $f < 1.5$ rev day^{-1}). Then, we applied these detection rates to debias our result with intervals of $\Delta m = 0.1$ mag, $f = 0.5$ rev day^{-1}, and $m = 0.5$ mag. It is worth noting that the triaxial ellipsoid used in the simulation could not fully represent the sophisticated asteroid shape, which would overestimate the detecting rate especially for low-amplitude object. However, including all possible asteroid shapes in such a simulation to investigate the biases from various factors in a detailed manner would becomes a formidable computing process that is far beyond the scope of this study. Our simulation could be the first step toward understanding whether the survey and the analysis tend to detect particular frequencies.

4.3. Statistical Analysis

4.3.1. Spin-rate Limit and Mean Spin Rate

To compare PTF results obtained both from this work and from Chang et al. (2014a), i.e., 1,751 PTF-U2s in total, with the objects of $U = 2$ in the LCDB, Figure 7 shows the plot of diameter versus rotation period for objects with the quality code $U = 2$. Because of our four-night observing time and limiting-magnitude range, most PTF-U2s are confined to the region $2 < P < 20$ hr and $1 < D < 10$ km, where most LCDB objects populate. The 2.2 hr spin barrier can clearly be seen for objects with $D > 150$ m, which indicates the spin-rate limit for rubble-pile asteroids under self-gravity. A small group of monolithic SFRs located at $D < 150$ m and $P < 2.2$ hr can survive fast rotation without breakup due to other mechanical forces besides self-gravity. In addition to 2001 OE84, we also found six large SFRs candidates, (320292) 2007 RO221, (334904) 2003 WL167, (335433) 2005 UW163, (337226) 2000 EL98, (346352) 2008 RM118, and 2006 AF62 (see Figure 4(z)), in which the super-fast rotation of 2005 UW163 has been confirmed (Chang et al. 2014b). While we plot the spin rate versus amplitude in Figure 8, all SFRs have bulk density $\rho > 3$ g cm^{-3} if $P \sim 3.3\sqrt{(1 + \Delta m)/\rho}$ is applied for rubble-pile asteroids, where Δm is the light-curve amplitude (Pravec & Harris 2000). Such high bulk density is very unusual among asteroids. The size-dependent strength model (Holsapple 2007) provides an alternative explanation, and we thus should observe a certain fraction of large SFRs. Although the five unconfirmed SFR candidates show reasonably good folded light curves, their super fast rotations still need to be verified by follow-up observations to exclude the possibility of noise-induced false-positive detections (Harris et al. 2012). If the SFR population is consistent with the overall asteroid spin-rate distribution, then we can rule them out as a distinct asteroid group.

The inset plot of Figure 7 is a detailed view of the dense region where the regressions of the spin rate for PTF-U2s and LCDB are computed using locally weighted scatterplot smoothing (Cleveland 1979). Both regressions share a similar trend that is flat for small asteroids and then gradually changes to longer rotation periods for larger asteroids.

4.3.2. Spin-rate Distribution

The spin-rate distribution for small asteroids is important for understanding the evolution of asteroid systems. At the moment, the available catalogs with large data volume include Pravec et al. (2008), Masiero et al. (2009, hereafter, M09), and LCDB. Pravec et al. (2008) have been collecting asteroid spin rates for more than a decade; therefore, the version of 2014 April 20 of their data set containing 462 asteroids is used in the following analysis (hereafter, P08, update 2014 April 20; private communication). We also include PTF-Ps in the spin-rate distribution of PTF-U2s by doubling their derived rotation

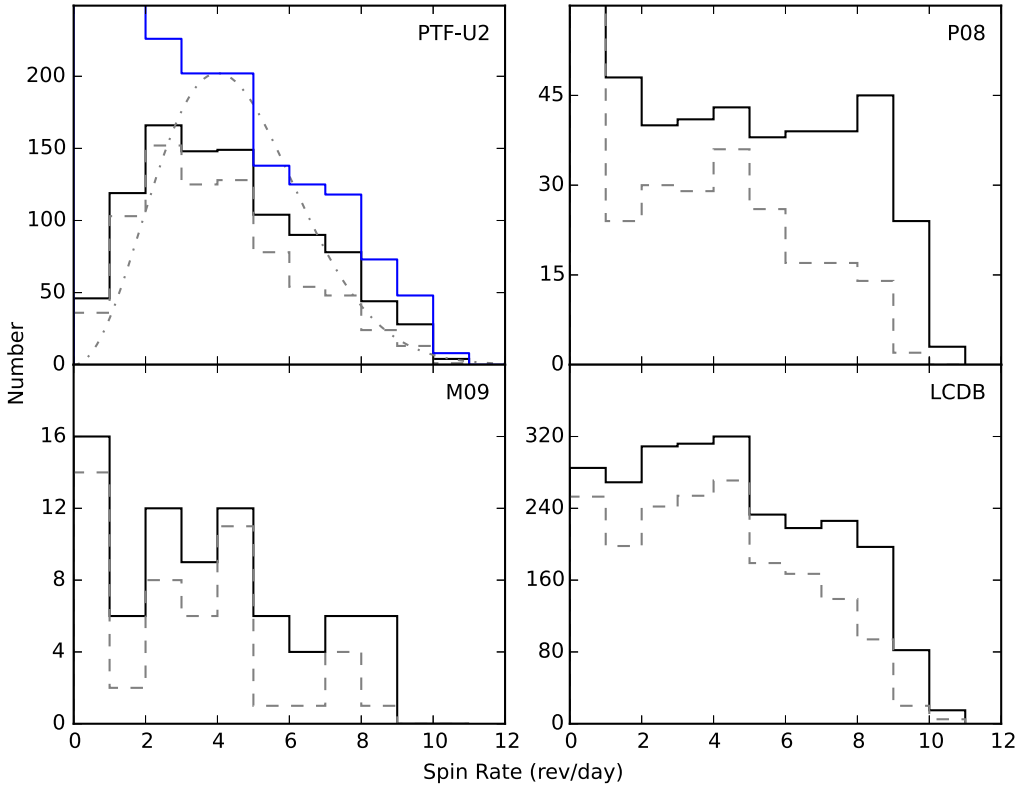

Figure 9. Spin-rate distributions of D3-15 asteroids for PTF-U2s, P08 (update 2014 April 20), M08, and LCDB. The gray dashed lines represent asteroids of $\Delta m > 0.2$ mag, the gray dot–dashed line on the plot for PTF-U2s is the best-fit Maxwellian distribution, and the blue line is the debiased result for PTF-U2s. Note that P08 (update 2014 April 20) is not in full scale.

period as suggested by their folded light curve. Approximately 95% of them are $f \leqslant 2$ rev day^{-1}, and the contribution of the rest is is very limited with respect to the whole PTF-U2s. In addition, the detection simulation does not pick up the "PTF-P"-like objects which result in an underestimated detection rate for $f \leqslant 2$ rev day^{-1}, and consequently an overestimation for long-period asteroids in the debiased result. Therefore, these two bins have such relatively large uncertainties that we see them as a reference and do not consider them in the following discussion.

To have a diameter range compatible with P08 (update 2014 April 20), we use asteroids of $3 < D < 15$ km (hereafter, D3-15) to compare the spin-rate distributions in Figure 9. In contrast to P08 (update 2014 April 20), none of the PTF-U2, M08, or LCDB objects have a flat distribution, which is quasi-Maxwellian for PTF-U2s (i.e., a peak at $3 \leqslant f \leqslant 5$ rev day^{-1} and a slow decrease after) and looks like a step function with a number decrease at $f = 6$ rev day^{-1} for M09 and LCDB. With debiased PTF-U2s, we cannot obtain a distribution as flat as P08 (update 2014 April 20) and the number decrease still remains. When these samples are divided by $\Delta m = 0.2$ mag, the spin-rate distributions become more consistent with each other for asteroids with $\Delta m > 0.2$ mag (i.e., quasi-Maxwellian). To invetigate this further, we separate them into the inner- ($2.1 < a < 2.5$ AU), mid- ($2.5 < a < 2.8$ AU) and outer- ($a > 2.8$ AU) main belt for detail investigation. Note that M09 is no longer included in the following analysis due to its insufficient number of samples for finer parameter space. Figure 10 shows that the difference between P08 and the others is mainly due to asteroids with $\Delta m < 0.2$ mag, where P08 (update 2014 April 20) has relatively more fast rotators (i.e., $f \geqslant 6$ rev day^{-1}). We believe that this discrepancy could be primarily due to the different survey strategies used, as pointed out by Masiero et al. (2009). However, this necessitates a more comprehensive study. Although the quasi-Maxwellian distribution could possibly be an observational bias caused by a greater detecting ability $2 \leqslant f \leqslant 5$ rev day^{-1} (Harris et al. 2012), we do not see this situation in the spin-rate distributions for various intervals of Δm (i.e., roughly flat for asteroids with $\Delta m < 0.2$ and $0.2 < \Delta m < 0.4$ mag). Moreover, most asteroids with $\Delta m \geqslant 0.4$ mag are $2 \leqslant f \leqslant 5$ rev day^{-1} and only a few at $f \geqslant 6$ rev day^{-1}. This is consistent with lower spin-rate limit for large-amplitude asteroids (see Figure 8). Furthermore, our detection simulation shows a roughly fair detection rate for $f > 2$ rev day^{-1}. This indicates that the quasi-Maxwellian distribution for D3-15 asteroids is not a result of favoring the detection of asteroids of $2 \leqslant f \leqslant 5$ rev day^{-1}.

When we look at the spin-rate distribution of asteroids with $D < 3$ km in Figure 11, we note an obvious decrease at $f = 6$ rev day^{-1} both in PTF-U2s and debiased PTF-U2s. This number drop still remains when applying an amplitude limit of $\Delta m > 0.2$ mag. Since the YORP effect timescale is relatively shorter for asteroids of $D < 3$ km and, moreover, the spin-rate limit is lower for large-amplitude asteroids, we believe that more large-amplitude asteroids of $D < 3$ km have been spun up to reach their spin-rate limit and broken up when compared with D3-15 asteroids, which results in a number decrease at $f = 6$ rev day^{-1}. Note that the small numbers at $f < 3$ rev day^{-1} in PTF-U2s are due to the lower detection

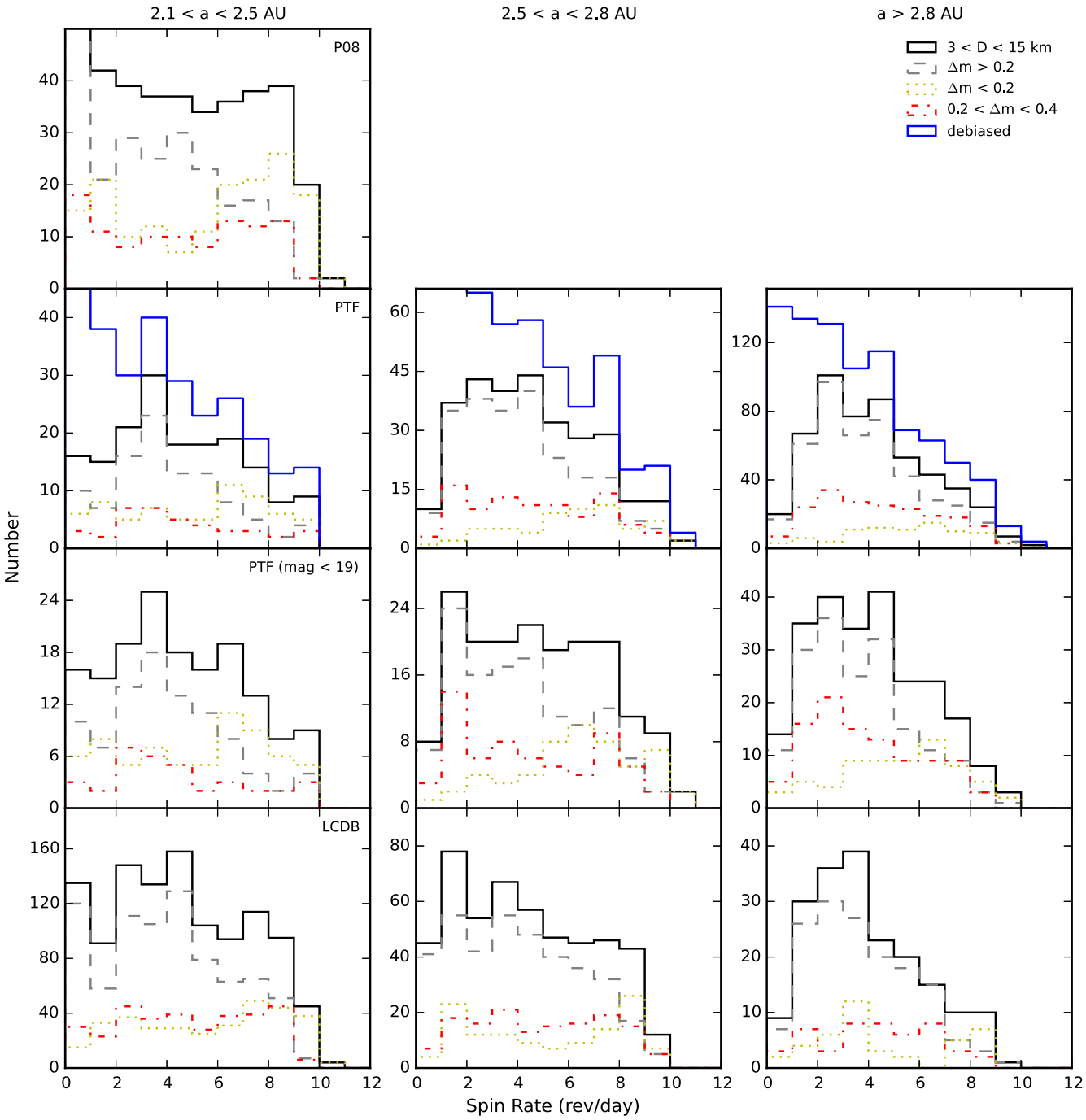

Figure 10. Spin-rate distributions of D3-15 asteroids (black line) in the inner- (left), mid- (middle) and outer- (right) main belts for P08 (update 2014 April 20; first row), PTF-U2s (second row), PTF-U2s with magnitude <19 mag (third row), and LCDB (last row). The blue solid, gray dashed, yellow dotted, and red dot–dashed lines represent debiased PTF-U2s, asteroids with $\Delta m > 0.2$, $\Delta m < 0.2$, and $0.2 < \Delta m < 0.4$ mag, respectively.

rate for small asteroids with long period. However, this deficiency becomes more comparable after debiasing.

Our result is not affected much by applying a brighter limiting magnitude of 19 mag (see bottom rows in Figures 10 and 11), such that our conclusion remains the same.

4.3.3. Spin Rate Versus Spectral Type

In PTF-U2 and LCDB data sets, there are 478 C-type, 928 S-type, and 136 V-type asteroids according to SDSS colors. When we look at the plot of diameter versus rotation period (left panel in Figure 12) and the plot of spin rate versus light-curve amplitude (middle panel) for the C, S, and V types (upper, middle, and lower panels, respectively), we see that they all occupy similar regions in rotation-period or spin-rate spaces. Because of the limiting magnitude of the observations and the various geometric albedo values involved, the asteroids have different diameter ranges. We note that C- and V-type asteroids seldom have objects with $P > 100$ hr and $P > 20$ hr, respectively. We see that the S and V types show clear boundaries at $\rho = 2\,\mathrm{g\,cm^{-3}}$, and the C type seems to have a boundary at $\rho = 1.5\,\mathrm{g\,cm^{-3}}$ with a small group extending to $\rho = 2\,\mathrm{g\,cm^{-3}}$. Therefore, the C-type asteroids have much fewer objects with $f > 8\,\mathrm{rev\,day^{-1}}$. Since M-type and E-type

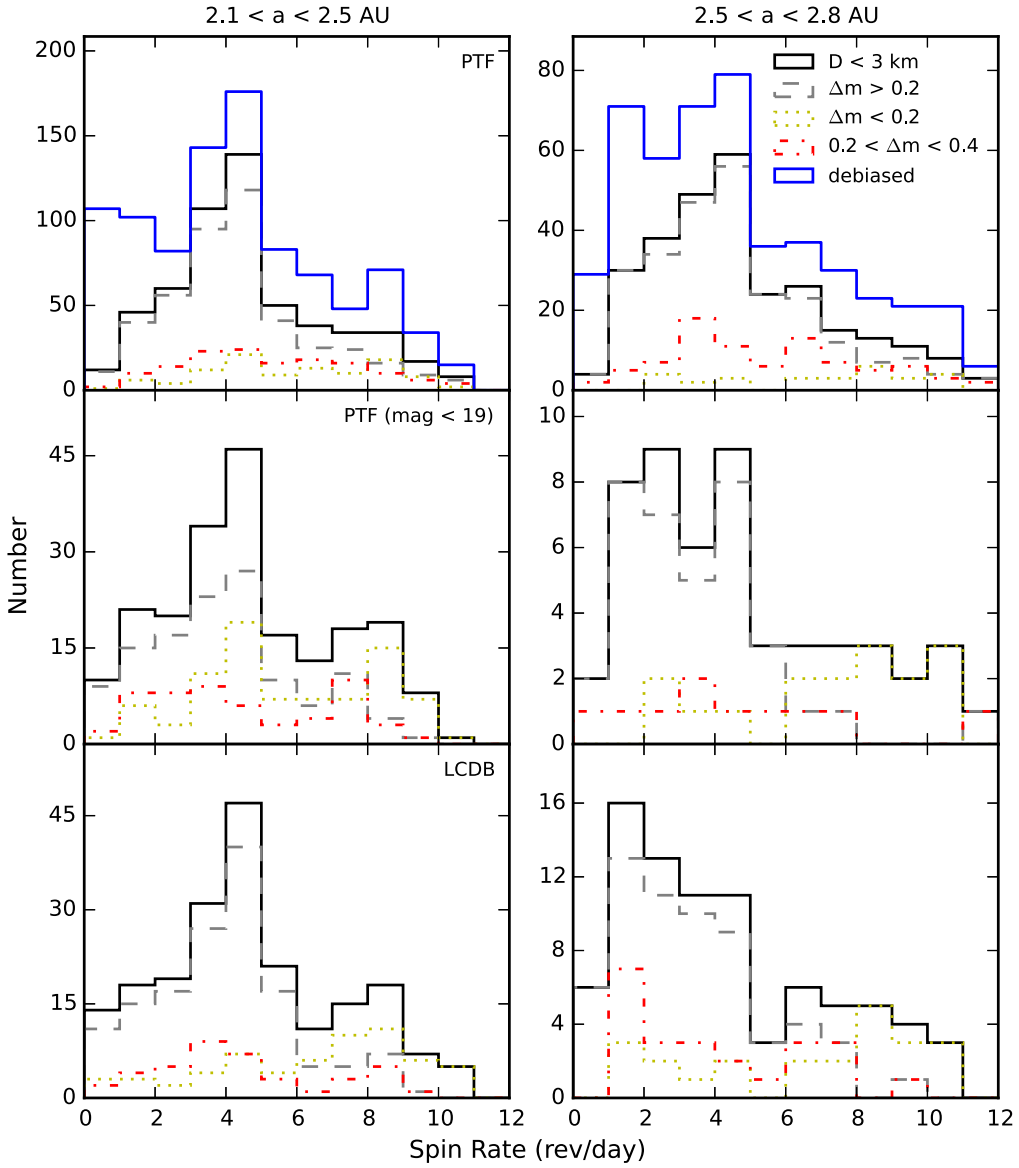

Figure 11. Spin-rate distributions of asteroids with $D < 3$ km. Same as Figure 10.

asteroids cannot be separated from C-type asteroids by SDSS colors, the small group in the C-type asteroids is properly due to those indistinguishable M- and E-type asteroids which have larger bulk density with respect to the C type. Despite the small group of C types, what we see here is in good agreement with the general sense of a lower bulk density for C types relative to S/V types. For a comparison without possible incompleteness at the large/small ends, we controlled our samples in the range of $3 < D < 20$ km to generate spin-rate distributions for these three asteroid types (right panel of Figure 12), in which there were 229, 657, and 81 objects, respectively. The overall shapes do not appear to be the same, but all of the distributions peak at $2 \leqslant f \leqslant 5$ rev day^{-1}. Besides, the C-type distribution is more Maxwellian-like. The Kolmogorov-Smirnov test on the spin-rate distribution gives p-values of 0.01, 0.003, and 0.026 for each pairing of CS, CV, and SV types, respectively. This indicates that their spin-rate distributions might be different from each other. However, this preliminary study needs to be confirmed when the samples are more complete in the parameter space.

5. SUMMARY

Two surveys of asteroid rotation periods have been carried out using the iPTF in 2014 January 6–9 and February 20–23. We obtained 1438 rotation periods from this campaign with quality codes $U \geqslant 2$, and most of them are associated with main-belt asteroids. There are 53 survey objects that match objects in the LCDB, and the derived rotation periods between these data sets are mostly in good agreement, an indication that our analysis is reliable.

By integrating this result with our previous study (Chang et al. 2014a), we found that the spin-rate distributions for D3-15 asteroids from PTF-U2s, M09, and LCDB are quasi-Maxwellian, which show number decrease with frequency for $f > 5$ rev day^{-1}. The discrepancy between P08 (update 2014

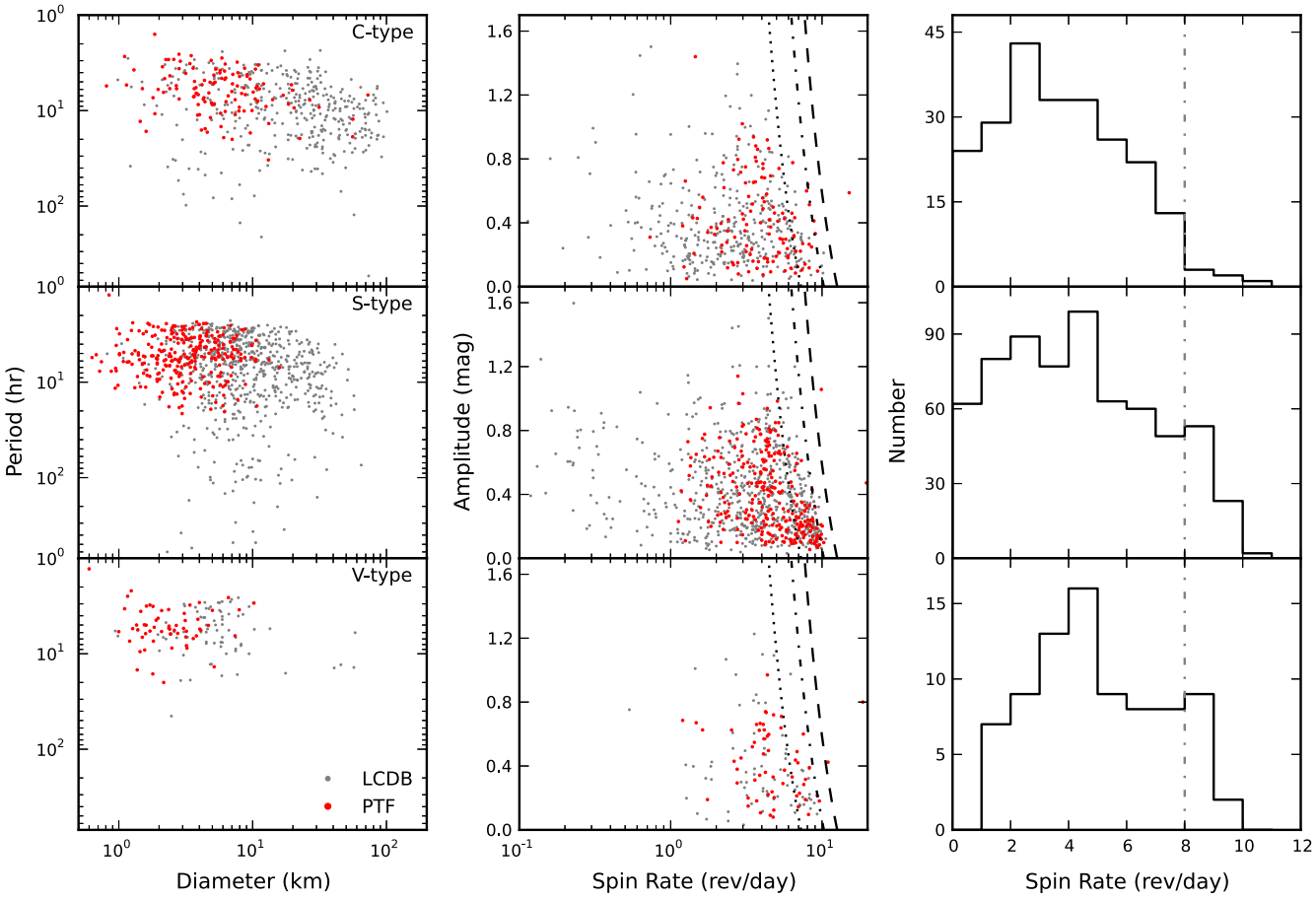

Figure 12. Asteroid rotation period vs. diameter (left), light-curve amplitude vs. spin rate (middle), and spin-rate distribution (right) for C- (upper), S- (middle), and V-type (lower) asteroids. The gray and red filled circles are LCDB objects and PTF-U2s, respectively.

April 20) and the others is mainly from asteroids with $\Delta m < 0.2$ mag and is probably due to different approaches toward acquiring samples of asteroid rotation periods. In addition, we found a significant number drop at $f = 6$ rev day^{-1} for asteroids of $D < 3$ km. This might be explained by the YORP effect, which works faster on small asteroids and pushes those elongate objects over their lower spin-rate limit to create the number drop at $f = 6$ rev day^{-1}.

Along with a confirmed large SFR, 2005 UW163 (Chang et al. 2014b), we also found five other SFR candidates. If $P \sim 3.3\sqrt{(1+\Delta m)/\rho}$ is followed for these asteroids, then their bulk densities are all much larger than 3 g cm^{-3}. This suggests that cohesiveness and tensile strength, in addition to self-gravity, should also play roles in keeping them from breaking apart under such fast rotation.

With the available SDSS colors, C-, S-, and V-type asteroids might have different distributions. However, their Maxwellian-like distributions suggest that they still retain a certain degree of collisional equilibrium. Moreover, we note that evidence suggests that C-type asteroids have a lower spin-rate limit than the S types. This agrees with the general impression that C-type asteroids have a lower bulk density than the S-type asteroids.

This work is supported in part by the National Science Council of Taiwan under the grants NSC 101-2119-M-008-007-MY3 and NSC 102-2112-M-008-019-MY3. We thank the referees, Petr Pravec and Alan Harris, for their useful suggestions and comments to improve the content of the paper. This publication makes use of data products from *WISE*, which is a joint project of the University of California, Los Angeles, and the Jet Propulsion Laboratory/California Institute of Technology, funded by the National Aeronautics and Space Administration. This publication also makes use of data products from *NEOWISE*, which is a project of the Jet Propulsion Laboratory/California Institute of Technology, funded by the Planetary Science Division of the National Aeronautics and Space Administration. We gratefully acknowledge the extraordinary services specific to *NEOWISE* contributed by the International Astronomical Union's Minor Planet Center, operated by the Harvard-Smithsonian Center for Astrophysics, and the Central Bureau for Astronomical Telegrams, operated by Harvard University.

REFERENCES

Behrend, R., Bernasconi, L., Roy, R., et al. 2006, A&A, 446, 1177
Bowell, E., Hapke, B., Domingue, D., et al. 1989, in Proc. of Conf. Asteroids II (Tuscon, AZ: Univ. Arizona Press), 524
Chang, C.-K., Ip, W.-H., Lin, H.-W., et al. 2014a, ApJ, 788, 17
Chang, C.-K., Waszczak, A., Lin, H.-W., et al. 2014b, ApJL, 791, L35
Cleveland, W. S. 1979, J. Am. Stat. Assoc., 74, 829
DeMeo, F. E., & Carry, B. 2013, Icar, 226, 723
Descamps, P., Marchis, F., Michalowski, T., et al. 2007, Icar, 189, 362
Grav, T., Mainzer, A. K., Bauer, J., et al. 2011, ApJ, 742, 40
Grillmair, C. J., Laher, R., Surace, J., et al. 2010, adass XIX, 434, 28
Harris, A. W. 1996, in Lunar and Planetary Institute Science Conf. Abstracts Vol. 27 (Woodlands, TX: LPI), 49

Harris, A. W., Pravec, P., & Warner, B. D. 2012, Icar, 221, 226
Harris, A. W., Young, J. W., Bowell, E., et al. 1989, Icar, 77, 171
Hergenrother, C. W., & Whiteley, R. J. 2011, Icar, 214, 194
Higgins, D. 2011, MPBu, 38, 41
Holsapple, K. A. 2007, Icar, 187, 500
Jedicke, R., & Herron, J. D. 1997, Icar, 127, 494
Jewitt, D., Ishiguro, M., & Agarwal, J. 2013, ApJL, 764, L5
Lacerda, P., & Jewitt, D. C. 2007, AJ, 133, 1393
Lacerda, P., & Luu, J. 2003, Icar, 161, 174
Laher, R. R., Surace, J., Grillmair, C. J., et al. 2014, PASP, 126, 674
Law, N. M., Dekany, R. G., Rahmer, G., et al. 2010, Proc. SPIE, 7735, 77353M
Law, N. M., Kulkarni, S. R., Dekany, R. G., et al. 2009, PASP, 121, 1395
Mainzer, A., Grav, T., Bauer, J., et al. 2011, ApJ, 743, 156
Margot, J. L., Nolan, M. C., Benner, L. A. M., et al. 2002, Sci, 296, 1445
Masiero, J., Jedicke, R., Ďurech, J., et al. 2009, Icar, 204, 145
Masiero, J. R., Mainzer, A. K., Grav, T., et al. 2011, ApJ, 741, 68
Ofek, E. O., Laher, R., Law, N., et al. 2012a, PASP, 124, 62
Ofek, E. O., Laher, R., Surace, J., et al. 2012b, PASP, 124, 854
Polishook, D., & Brosch, N. 2009, Icar, 199, 319
Polishook, D., Ofek, E. O., Waszczak, A., et al. 2012, MNRAS, 421, 2094
Pravec, P., & Harris, A. W. 2000, Icar, 148, 12
Pravec, P., Harris, A. W., Vokrouhlický, D., et al. 2008, Icar, 197, 497
Pravec, P., Kušnirák, P., Šarounová, L., et al. 2002, Asteroids, Comets, and Meteors: ACM Vol. 500, ed. B. Warmbein (Noordwijk: ESA), 743
Pravec, P., Scheirich, P., Kušnirák, P., et al. 2006, Icar, 181, 63
Pray, D. P., Galad, A., Husarik, M., & Oey, J. 2008, MPBu, 35, 34
Rau, A., Kulkarni, S. R., Law, N. M., et al. 2009, PASP, 121, 1334
Rubincam, D. P. 2000, Icar, 148, 2
Salo, H. 1987, Icar, 70, 37
Tedesco, E. F., Cellino, A., & Zappalá, V. 2005, AJ, 129, 2869
Warner, B. D. 2014, MPBu, 41, 102
Warner, B. D., & Harris, A. W. 2011, Icar, 216, 610
Warner, B. D., Harris, A. W., & Pravec, P. 2009, Icar, 202, 134
York, D. G., Adelman, J., Anderson, J. E., Jr., et al. 2000, AJ, 120, 1579